應用重力及數值模擬研究區域地質構造
個案研究:新竹斷層、西南海域泥貫入體

Studying Geologic Structures in Lights of Gravity and Numerical Modelling
Case Study on Hsinchu Fault and Mud Diapirs Offshore Southwestern Taiwan

連紫猗 Tzuyi Lien

Institute of Oceanography, National Taiwan University

Partners:
Cheinway Hwang, David Crossley,
Emmy T.-Y. Chang,
Eh Tan,
CharShine Liu, LinagFu Lin, HsienHsiang Hsieh and WeiChung Han

2017.3.17

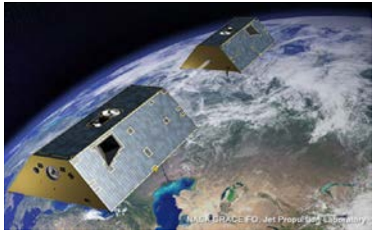

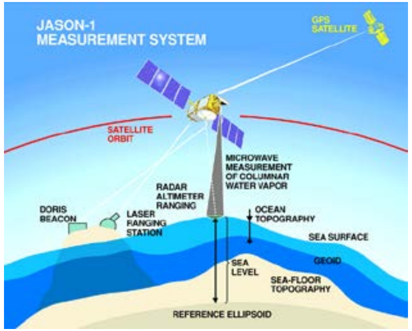

The state-of-the-art gravimetric observations:

GRACE

Satellite Altimetry

- Tectonic features in ocean basins(Sandwell etc)
- Ocean mass change

Absolute gravimeter: FG5

Relative gravimeter: CG5、EG、S130、SG

Superconducting Gravimeter (SG) Time-varying gravity

- High precision in determining the mass redistribution inside the Earth.
- Free oscillation of the earth, in particular triggered by the very big earthquakes.

Airborne/shipborne gravimeter (S130) Static gravity

Airborne/shipborne gravimeter (S130)

Static gravity

Superconducting Gravimeter (SG)

Time-varying gravity

mGal

nGal

$$g = 9.800000000 \ m/s^2$$

1 2 3 4 **5** 6 7 **8** 9

mGal=10^{-5} uGal=10^{-8}

Superconducting Gravimeter

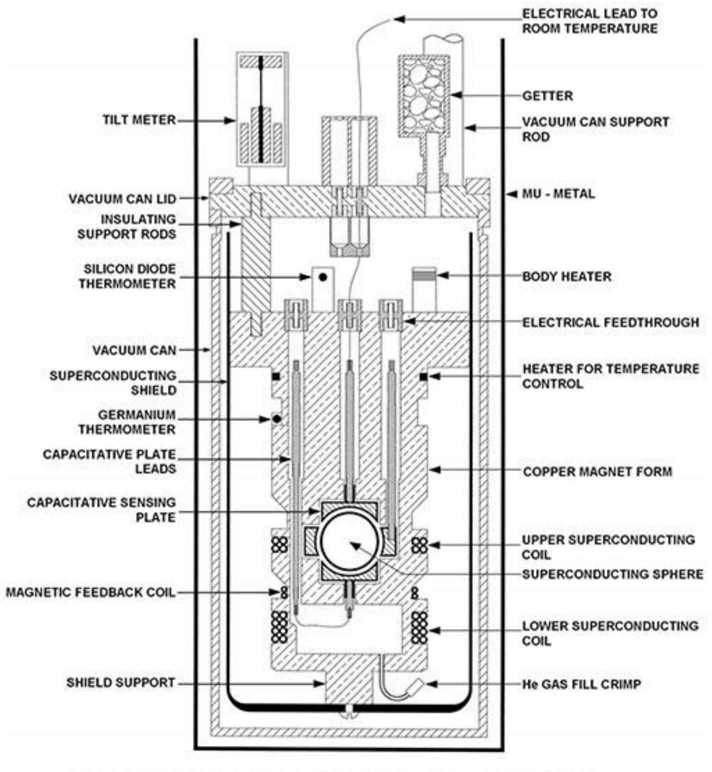

Gravity Sensing Unit
GWR website, http://www.gwrinstruments.com/)

Superconducting Gravimeter (SG T48)
in Hsinchu

Superconducting Gravimeter

Effect	Magnitude (µgal)	Frequency range	Method
Solid earth tide	Up to 300	12-24 hr (dominated)	DDW (Dehant et al., 1999)
Ocean tide loading	10	12-24 hr (dominated)	NAO.99b (Matsumoto et al., 2000)
Local atmospheric pressure	10	Minutes to seasonal	Standard model (Torge , 1989) using pressure data
Polar motion	5	Annual	Standard model (Torge, 1989) using IERS data
Non- local hydrology	0.5	Daily to annual	From GPP using GLDAS
Non- local atmospheric pressure	Up to 1.5	Minutes to seasonal	From GGP using ECMWF

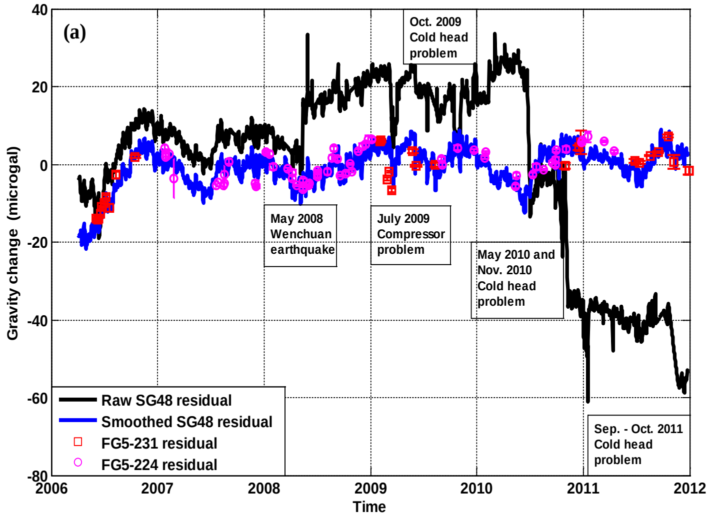

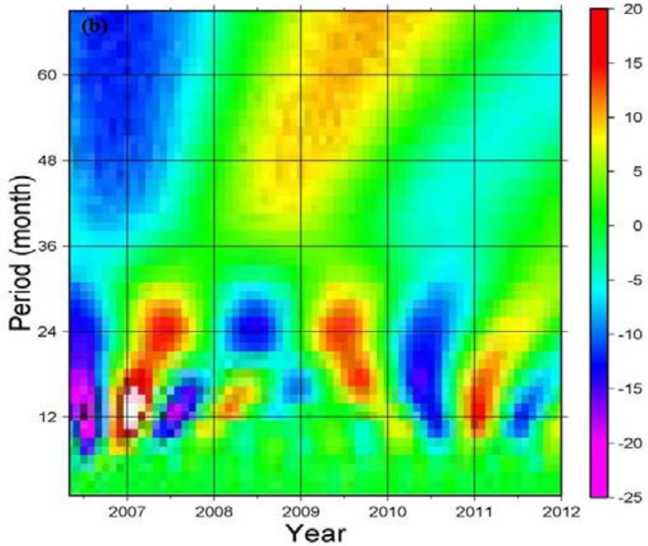

Groundwater modeling

- Governing groundwater flow equation is derived from **Darcy's law** and **continuity equation** (Bedient and Huber, 2002), and can be expressed as:

$$\frac{\partial}{\partial x}\left(K_x b\frac{\partial h}{\partial x}\right)+\frac{\partial}{\partial y}\left(K_y b\frac{\partial h}{\partial y}\right)+\frac{\partial}{\partial z}\left(K_z b\frac{\partial h}{\partial z}\right)-W=S\frac{\partial h}{\partial t}$$

where W is recharge/discharge, h head, b thickness of aquifer, S storage coefficient.

- In unconfined aquifer, storage coefficient is equal to specific yield (S_y), and the thickness of aquifer is equal to head.
- In confined aquifer, storage coefficient is $S=S_s b$ (S_s specific storage), and the thickness of aquifer is constant.

- Modular three-dimensional groundwater flow model (**MODFLOW**; Harbaugh et al., 2000)
- A program developed by the USGS for modeling 3D groundwater field
- Using block-centered finite-difference method to compute water head at each grid.

Model A: Without Fault

The modeled water levels north of the HF are too high, causing groundwater to discharge into the Touchien River more rapidly than the observations; the water should ideally stay on the south side of the study area.

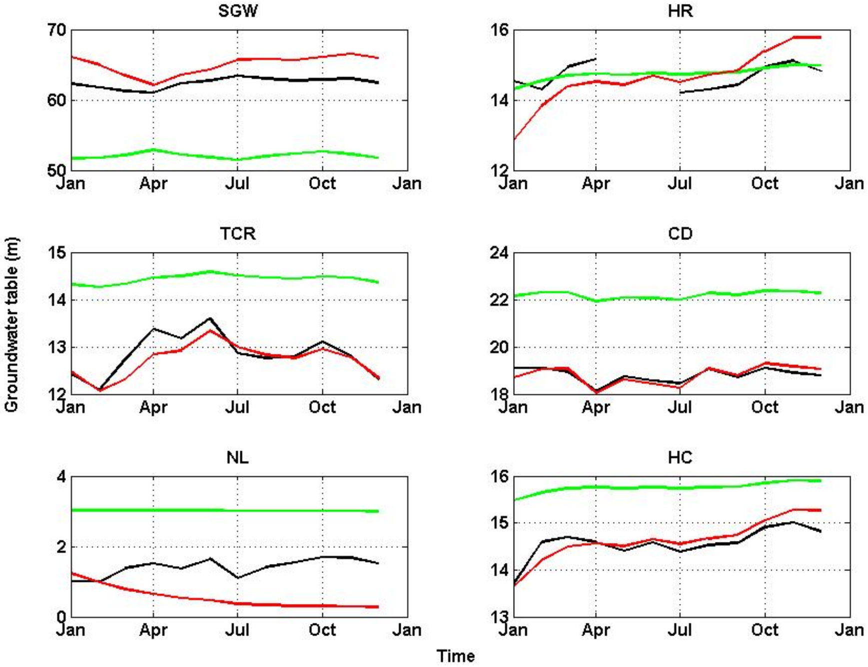

Observed groundwater tables (in black) with predictions from Model A (in green) and Model B (in red)

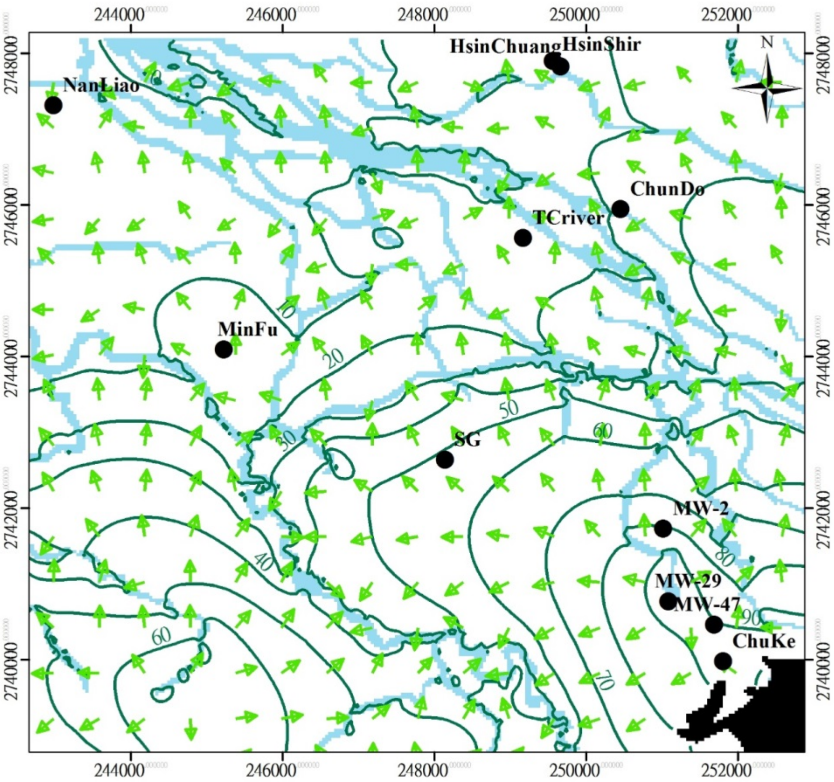

Hsinchu Fault (HF)

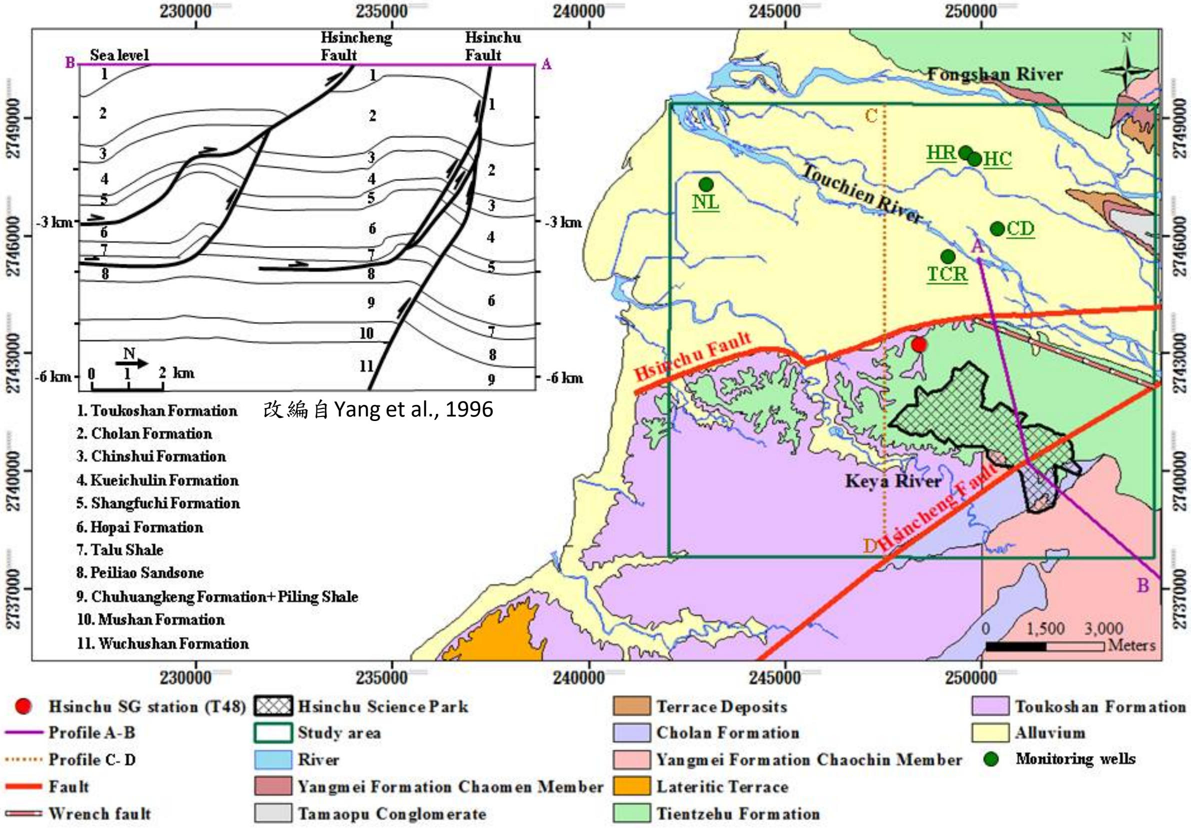

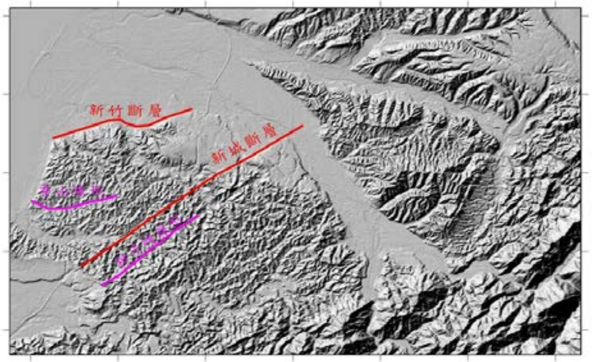

圖二 竹東丘陵區域數位地形圖（DTM）及活動斷層分布 From CGS report

- Almost none **outcrop** evidence found in field investigation [Tang, 1968]
- Very quiet in terms of **seismic** activity
- Surface deformation monitored by **GPS** did not find significant slip [Shea et al., 2011]
- Static **gravity** could not tell fault from folding [Pan, 1965]

- **Geomorphology** strongly suggested existence of fault [Chen et al., 2004]
- **Seismology** supported the existence of the fault [Yang et al., 1996]
- **Borehole** well data showed positive evidence (from CGS)

Impact of Fault-Imposed Boundary Condition on Groundwater Flow

Caine et al. [1996]

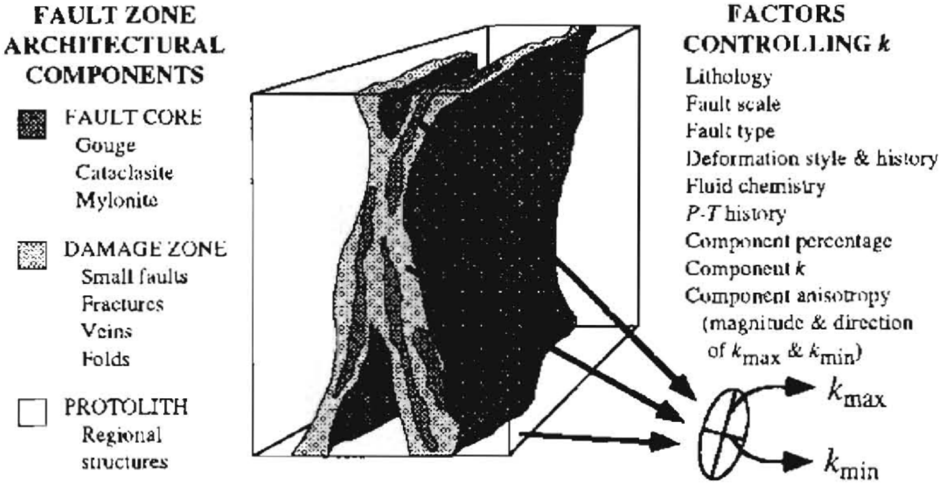

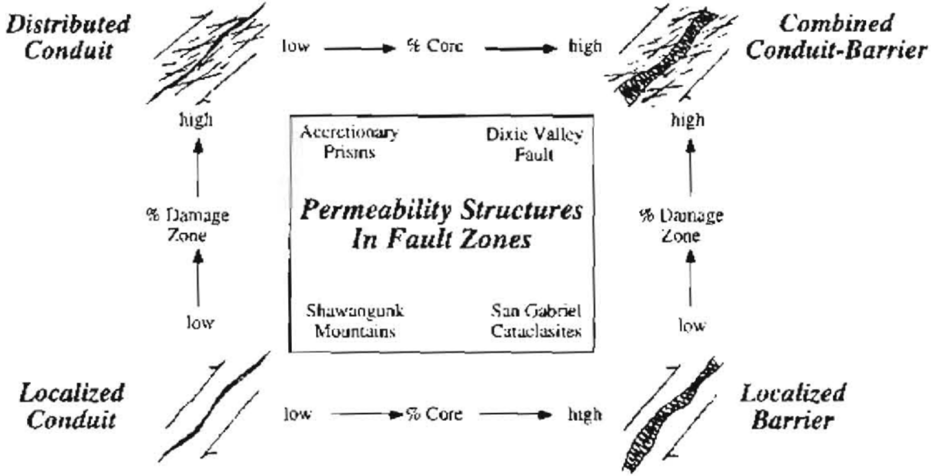

Impact of Fault-Imposed Boundary Condition on Groundwater Flow

Wibberley and Shimamoto [2003]

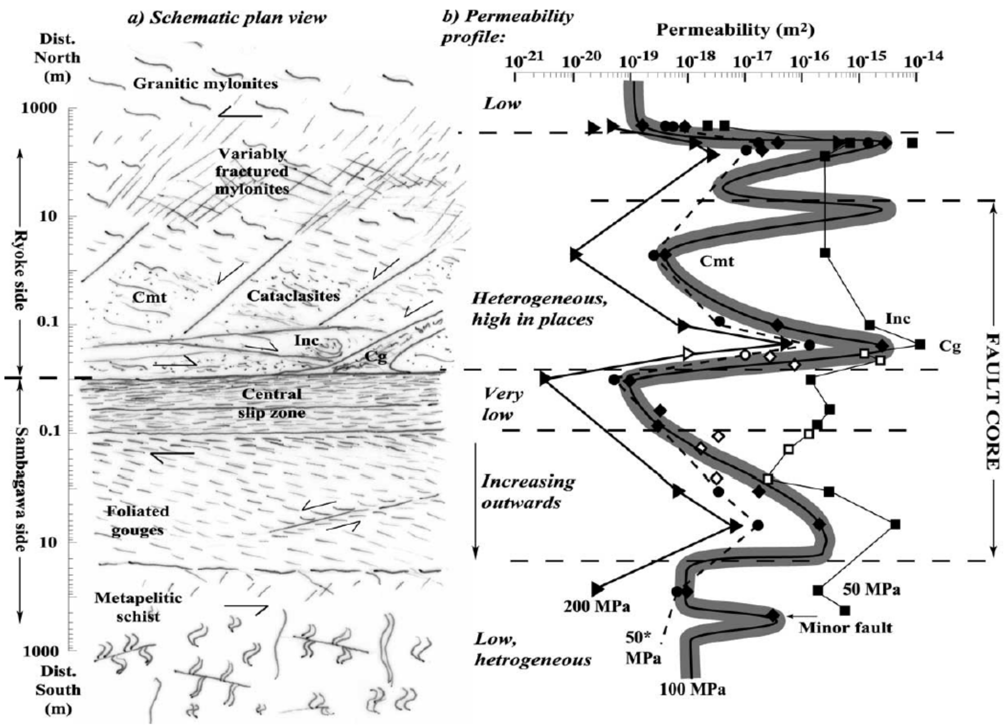

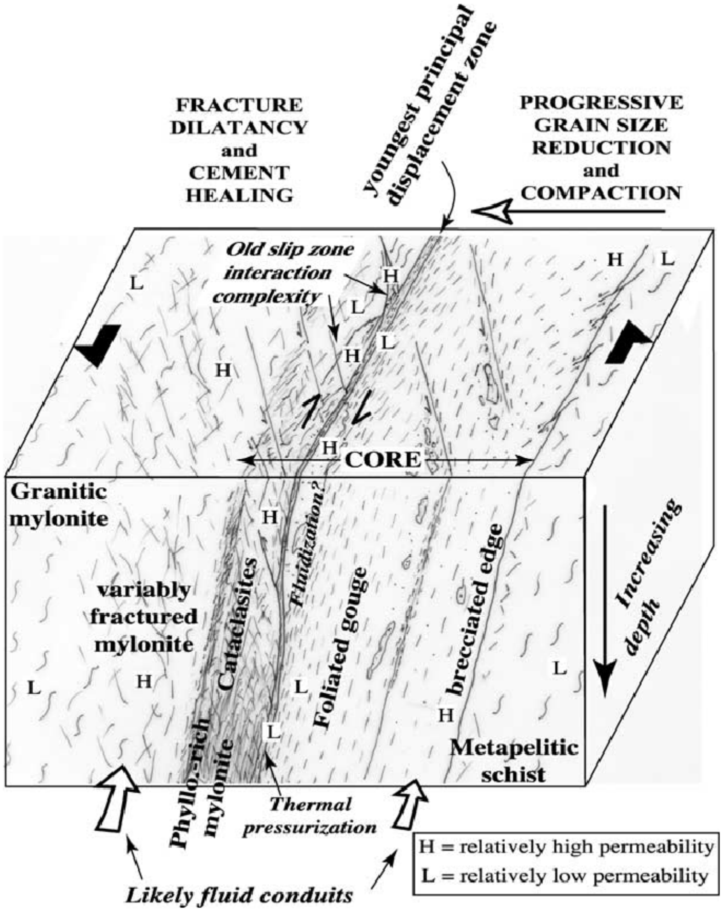

Impact of Fault-Imposed Boundary Condition on Groundwater Flow

Micarelli et al. [2006]

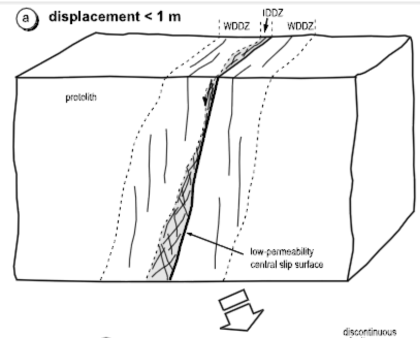

No fault core

Permeability decrease restricted to few millimetres of rock adjacent to the fault surface

- *Porosity reduction in the finest size fraction of the sediment*

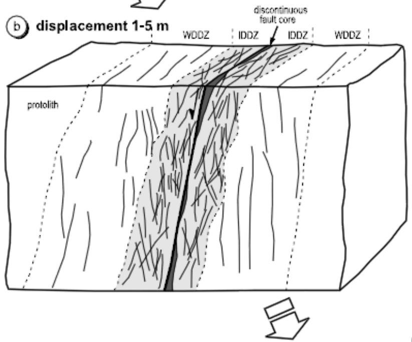

Discontinuous fault core with cataclasis onset

Permeability decrease within 1-2 cm of rock close to the fault surface

- *Porosity reduction in the finest size fraction of the sediment*
- *Empty fossil shell crushing*

Continuous fault core

Permeability decrease within first few centimetres close to the fault surface

- *Empty fossil shell crushing*
- *Rotation-enhanced particle abrasion*
- *Late precipitation of calcite cement*

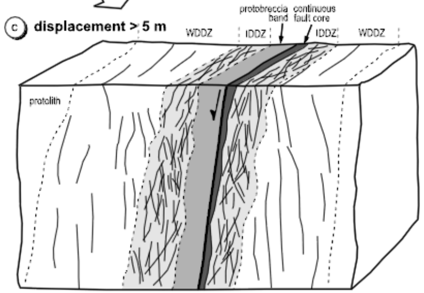

Impact of Fault-Imposed Boundary Condition on Groundwater Flow

Caine et al. [1996] showed that if a water-resistant core has been formed, a **decrease of conductivity** usually occurs in the direction **perpendicular to the fault plane**.

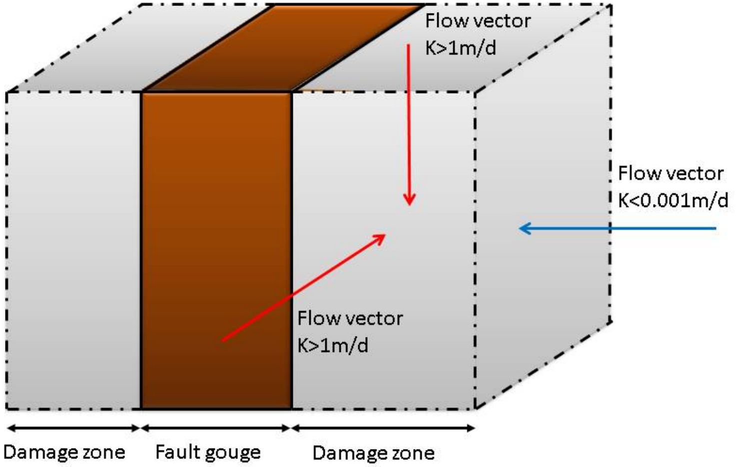

At a location where the water flow is **parallel to the fault plane**, the conductivity may increase due to the **increase in permeability** provided by the microfractures in the damage zone [Wibberley and Shimamoto, 2003].

改編自 Yang et al., 1996

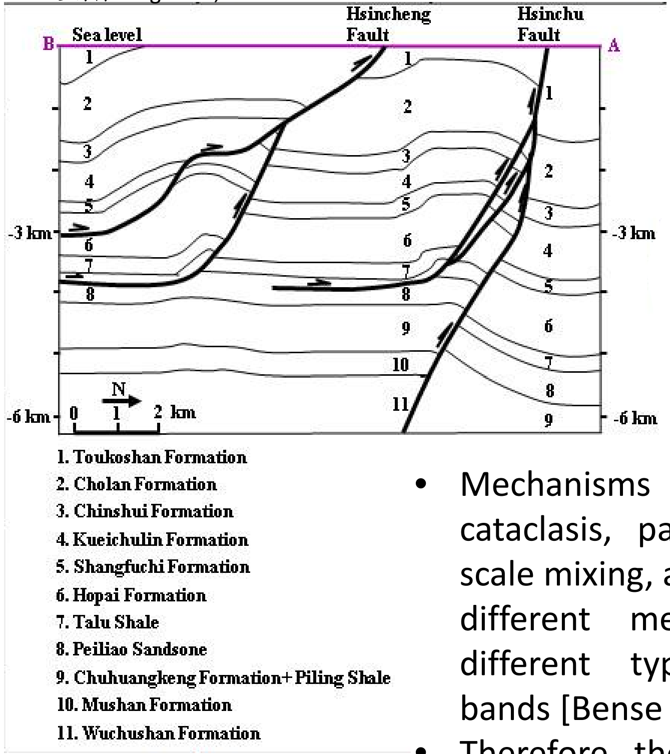

Micarelli et al. [2006] showed that the existence of a **fault core** is always associated with significant displacement of **slip**.

- Mechanisms of fault slips include cataclasis, particulate flow, grain-scale mixing, and clay smearing, and different mechanisms result in different types of deformation bands [Bense et al., 2003].
- Therefore, the existence of a fault core provides evidence that the underlying fault may be active.

Model B: With Fault

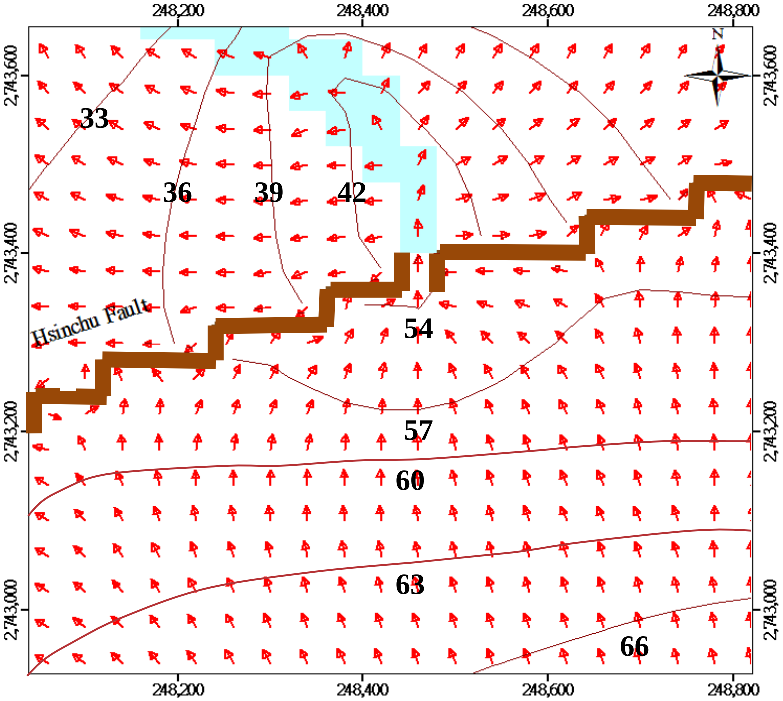

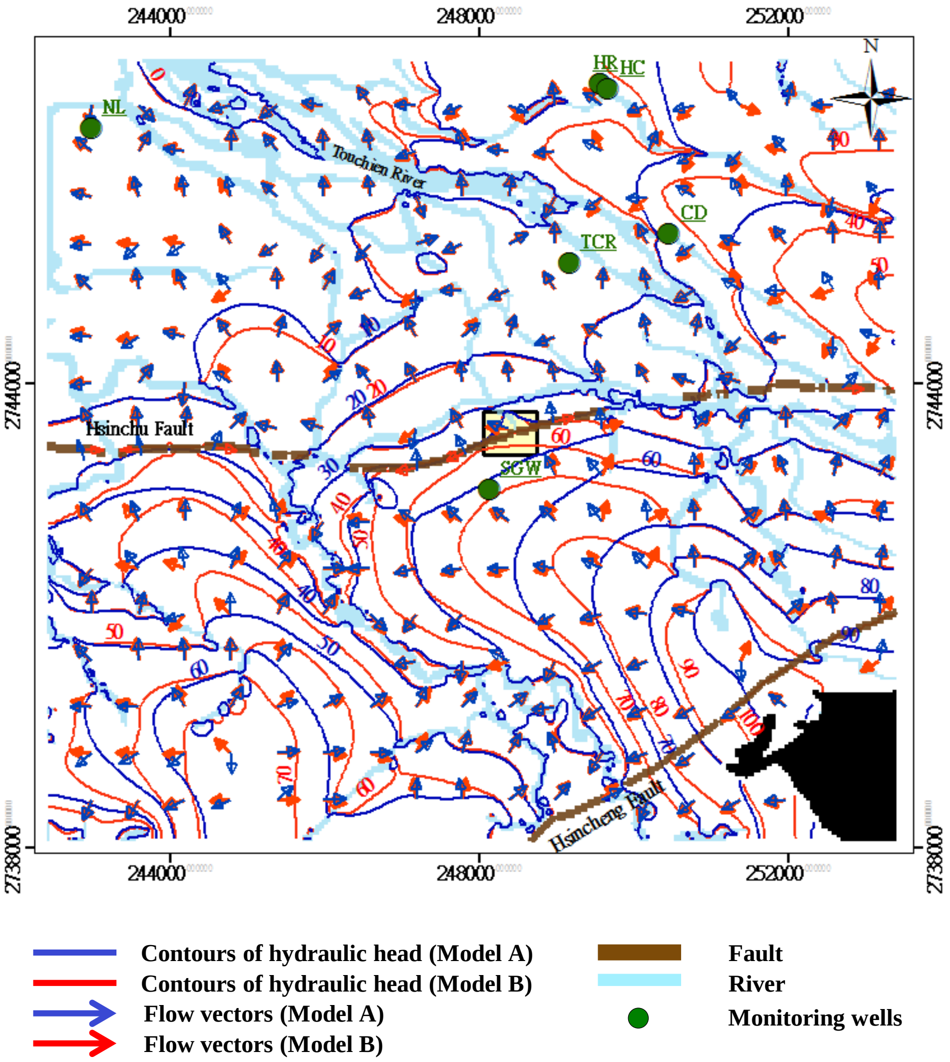

Model A & Model B

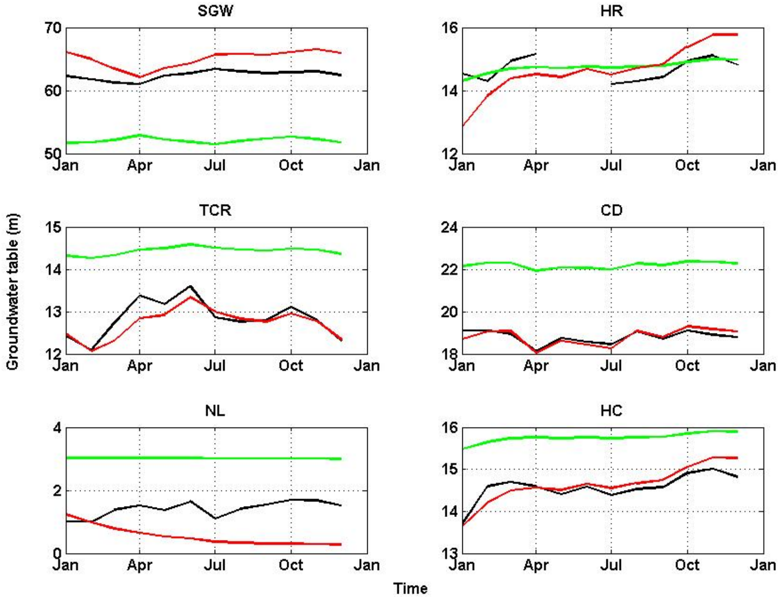

Observed groundwater tables (in black) with predictions from Model A (in green) and Model B (in red)

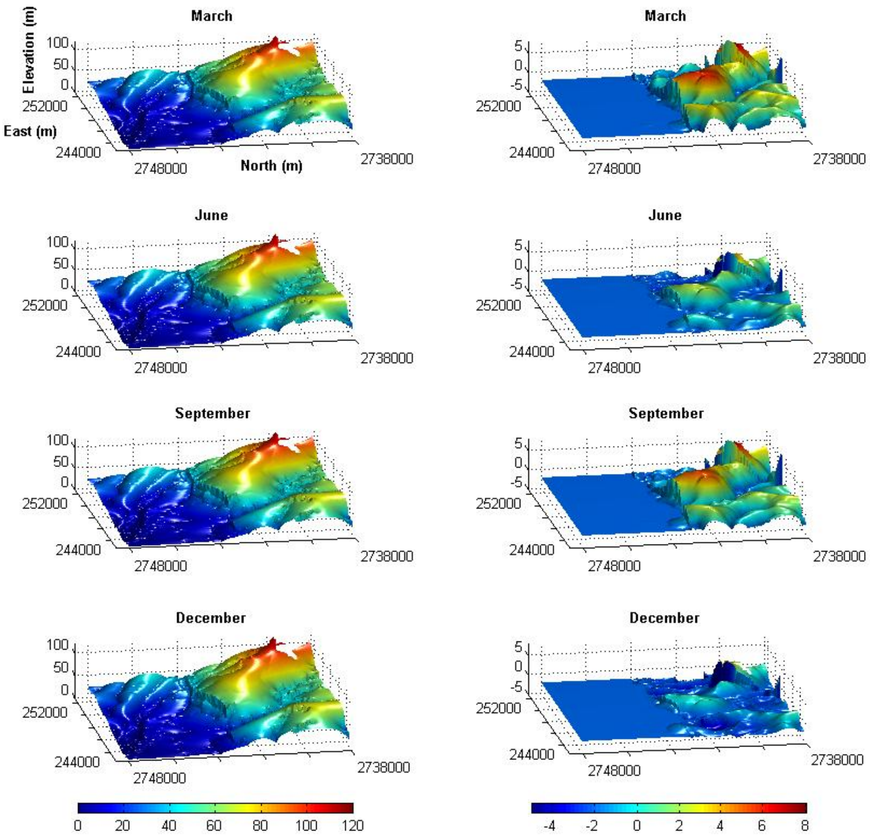

(left column) Hydraulic heads (unit: m) from Model A and (right column) the differences in hydraulic head between Model B and Model A in selected months.

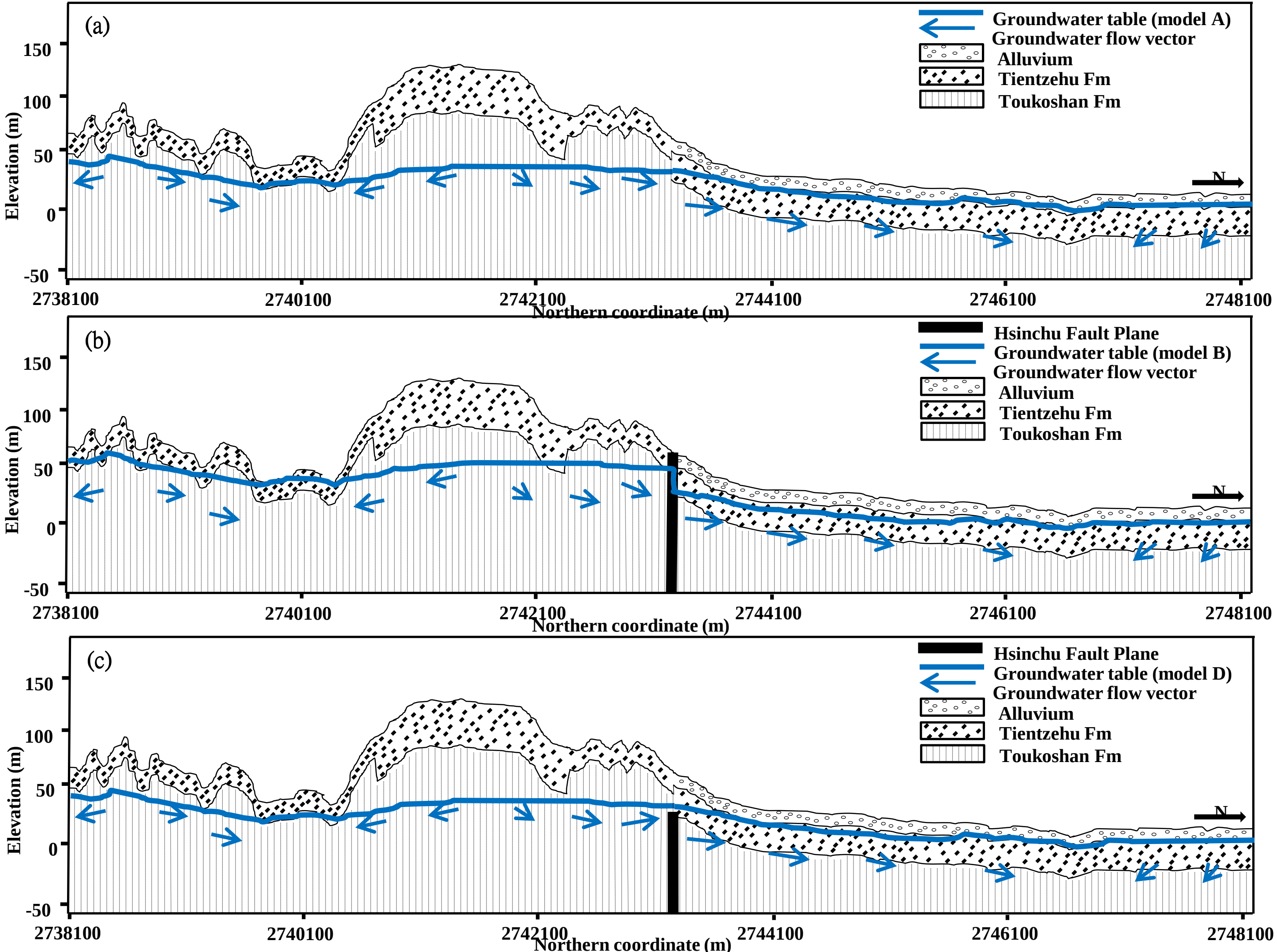

(a)
Groundwater table (model A)
Groundwater flow vector
Alluvium
Tientzehu Fm
Toukoshan Fm
N
Elevation (m)
150
100
50
0
-50
2738100
2740100
2742100
2744100
2746100
2748100
Northern coordinate (m)
(b)
Hsinchu Fault Plane
Groundwater table (model B)
Groundwater flow vector
Alluvium
Tientzehu Fm
Toukoshan Fm
(c)
Hsinchu Fault Plane
Groundwater table (model D)
Groundwater flow vector
Alluvium
Tientzehu Fm
Toukoshan Fm

Gravity Effects

- Gravity: sum of mass anomaly in space
  Groundwater well: limits of spacial distribution
- Monthly data is enough to define the result of gravity change due to water level and fault.

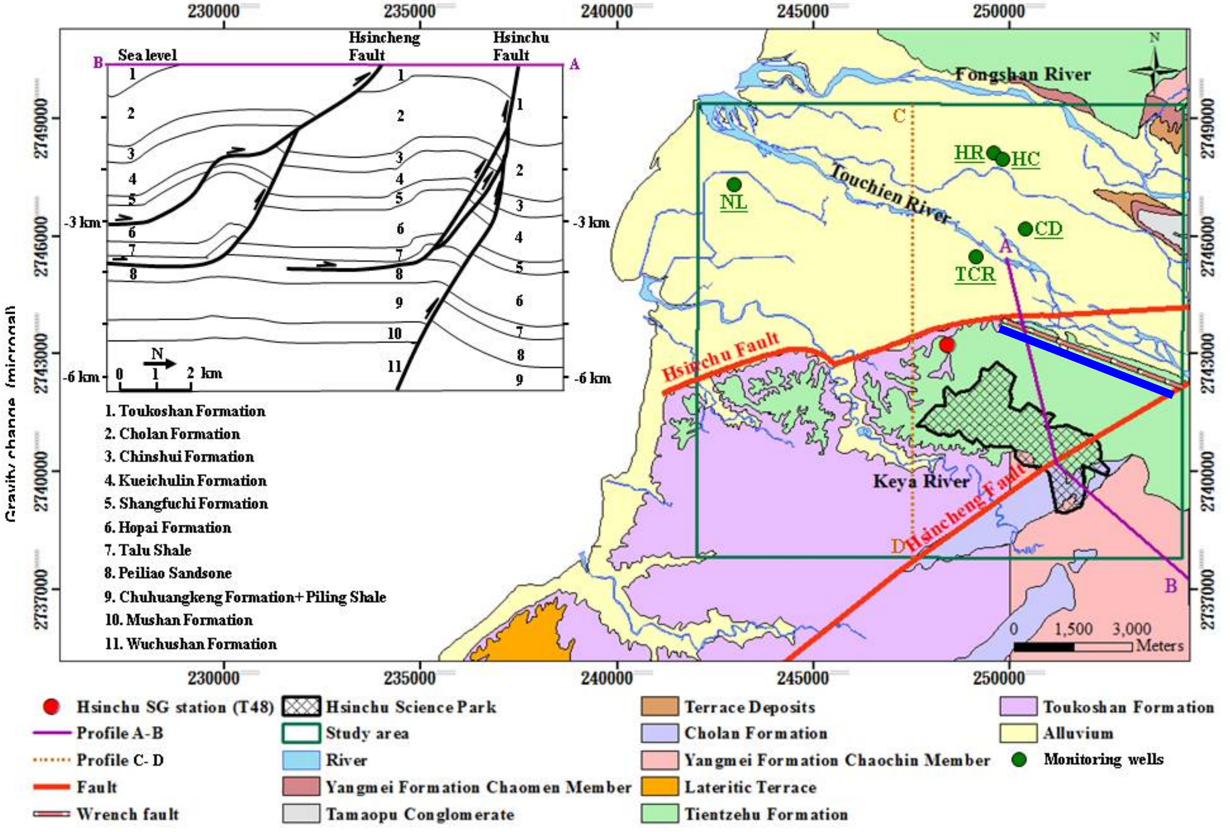

· effects in dry and wet seasons in one
e biggest contrast when assessing the

	Purpose	Inferences based on statistical test
e	to verify the existence of HF	Existence of HF is accepted
rth	to detect fault location	100 m shift to north is more likely than current HF location
	to test the top "opening" of HS fault to estimate latest seismic activity	most recent slip of HF can be dated to the beginning of Holocene
	to verify the existence of wrench fault	existence of wrench fault is inconclusive

Ocean Research I (ORI) shipborne gravity

since 2009 to the present

131 cruises

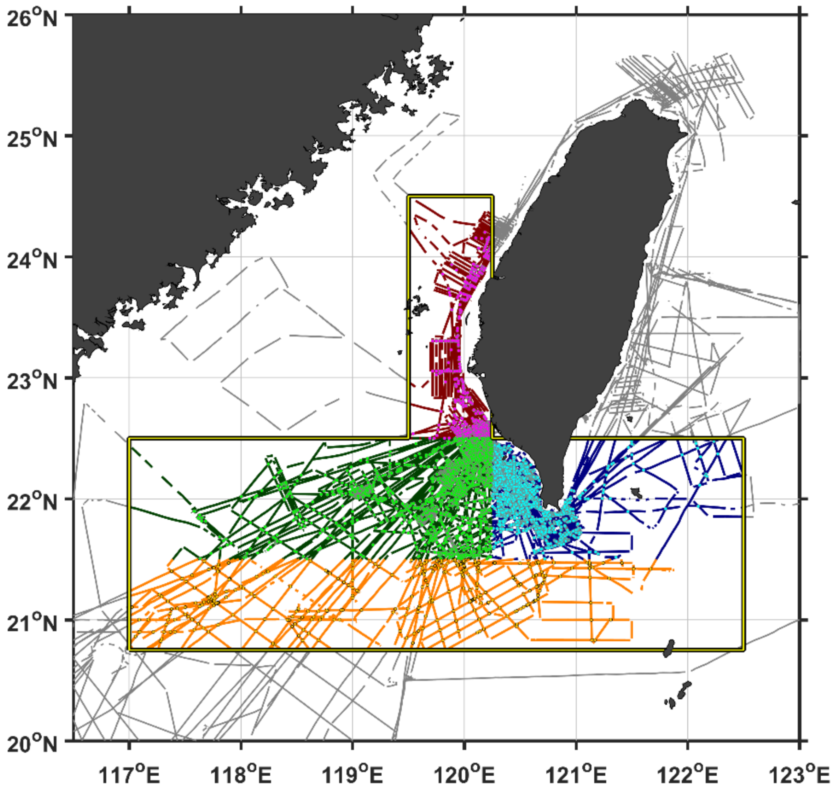

gravity data

Gravity data processing:
Ocean data bank

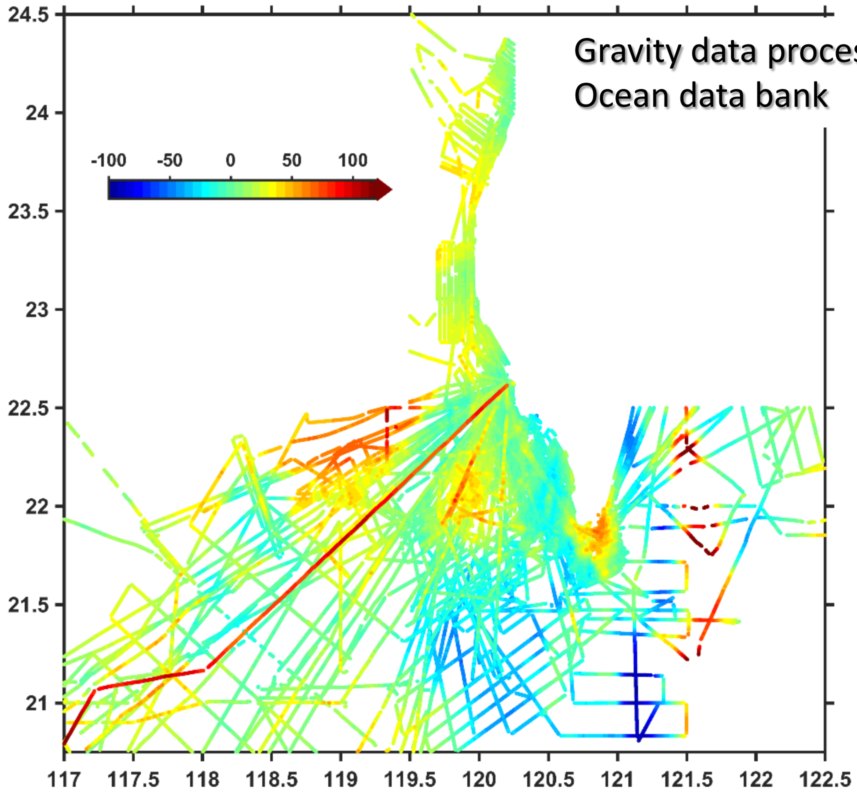

Free-air gravity anomaly related to topographic feature

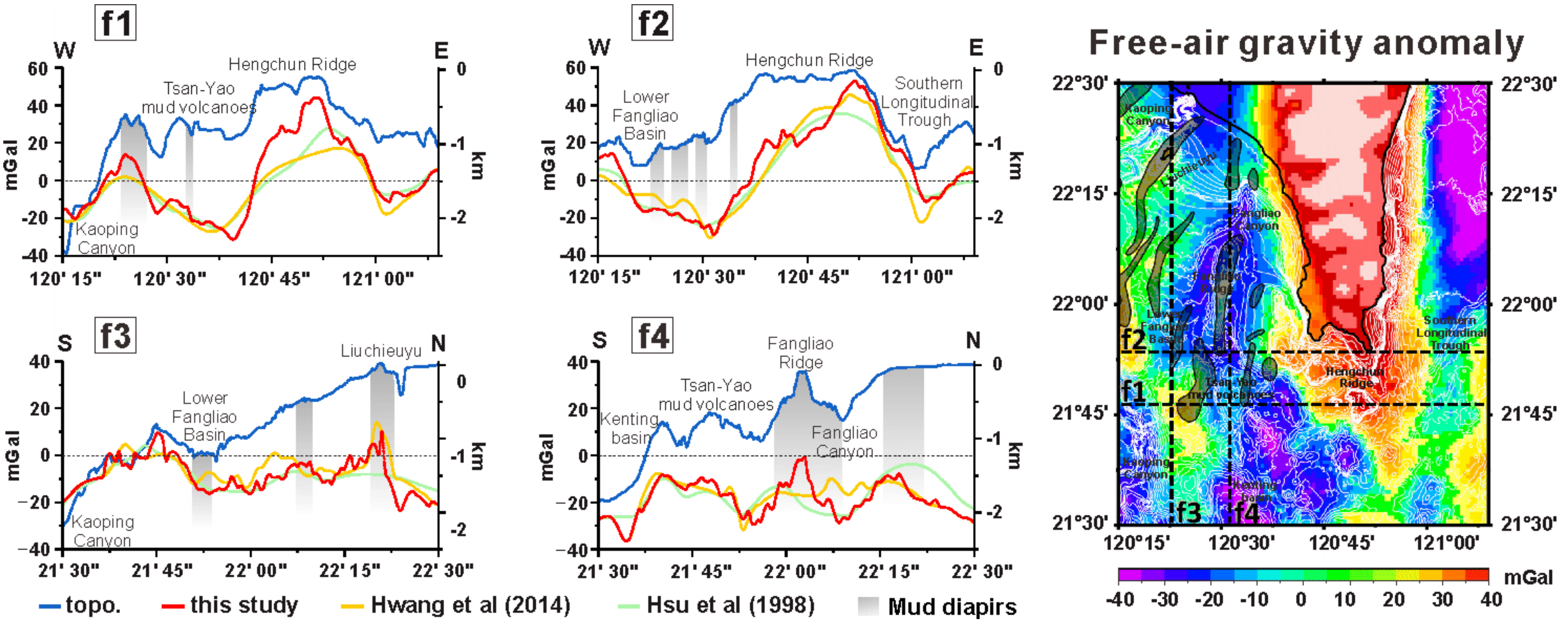

Distribution of mud diapirs: Chen, S.C., et al., 2014

No data area is filled by Hwang et al., 2014

Bouguer gravity anomaly

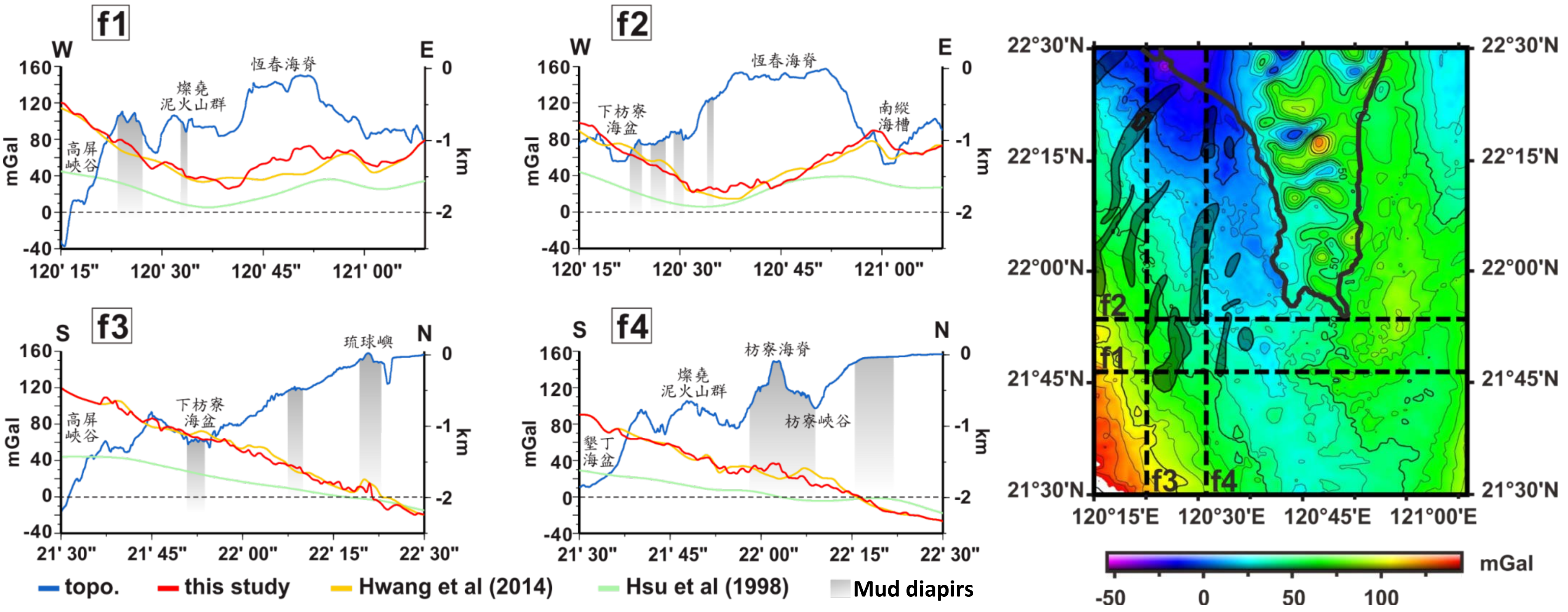

Bouguer gravity anomaly

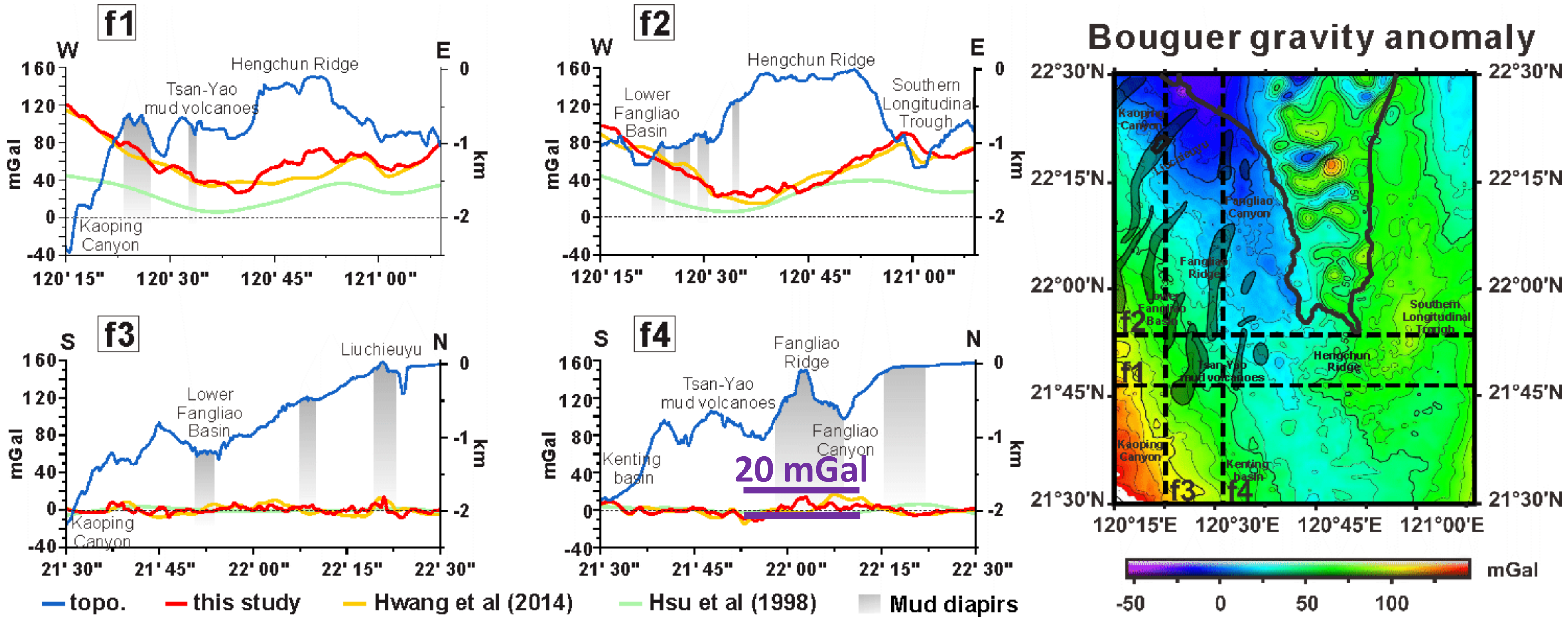

Lateral density anomaly

Surface Gravity Anomalies

Possible causes to have the “slightly” lateral density anomaly,

(1) Intrusion of fluid or mud diapir to the shallow strata. → negative gravity anomaly

(2) The convergent structures, folding, faulting, etc → positive gravity anomaly at folding axis or the raising of strata by fault

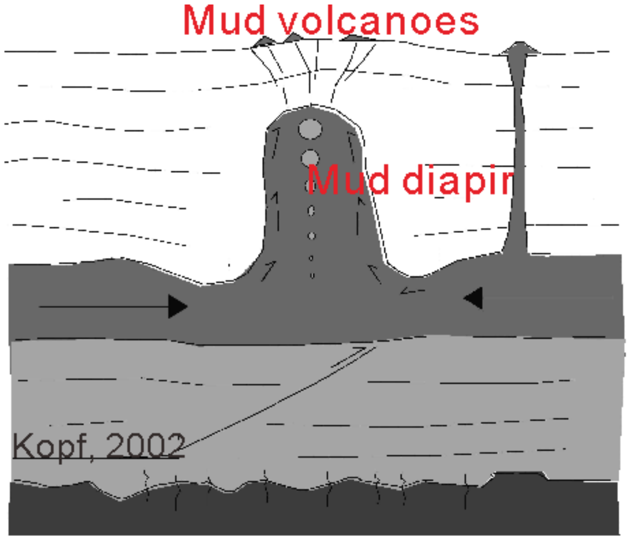

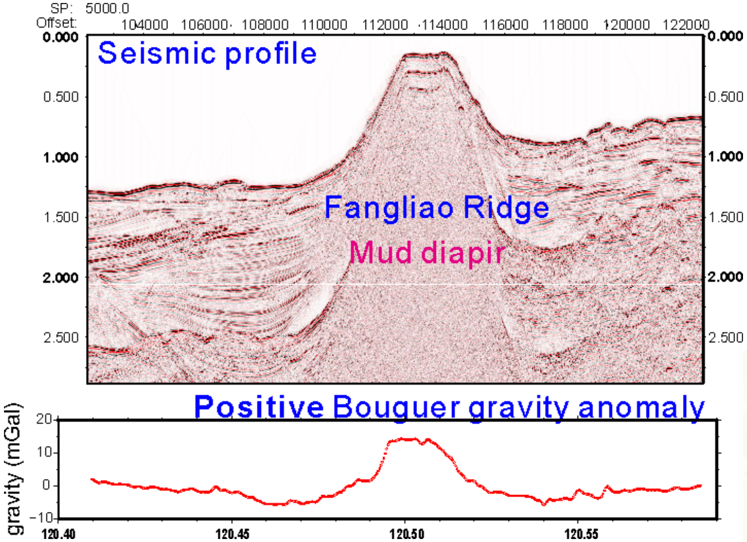

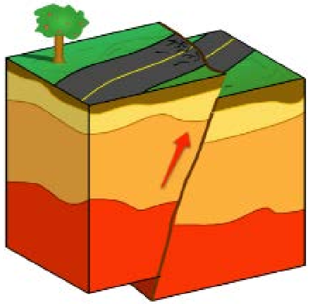

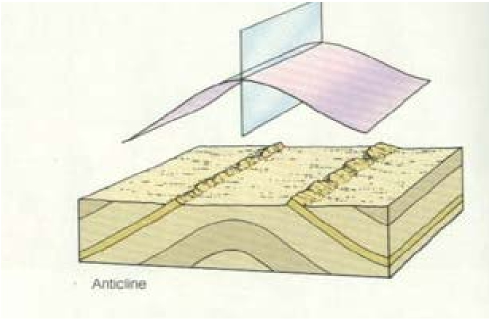

rapid sedimentation
low density deposit
Buoyancy force

convergent zone
tectonic stress

Tectonic deformation modelling - DynEarthSol2D

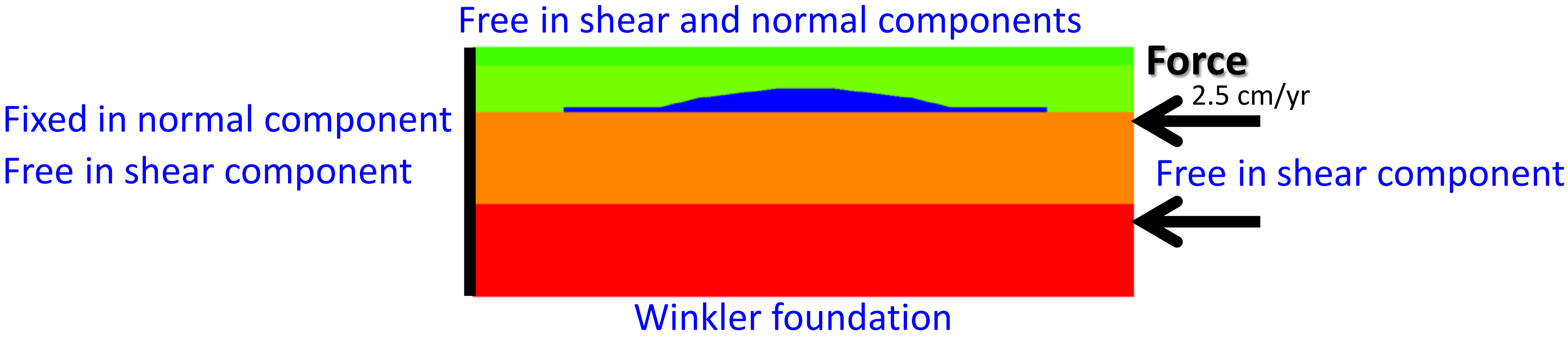

[Geometry design]
- length, width, height,
- layers

[Material parameters]
rheology type, number of materials, density, bulk modulus, shear modulus, viscosity, heat capacity, plastic strain, cohesion, friction angle

[Others]
temperature, erosion and sedimentation rate, water loading, weak zone

Convergent rate: 2.5 cm/yr
Rheology type : elasto-visco-plastic

	Sediment	Light/dense material	Oceanic crust
Density (kg/m^3)	2400/2460	1800/2460	2800
Bulk modulus (GPa)	20	8	50
Shear modulus (GPa)	6	3	30
Viscosity (Pa.s)	1e17	1e18	1e24
Plastic strain 0	0	0	0
Plastic strain 1	1	1	1
Cohesion 0 (MPa)	40	40	40
Cohesion 1 (MPa)	4	4	10
Friction angle 0 ($^\circ$)	10	10	30
Friction angle 1 ($^\circ$)	1	1	15

Geometry design

Two layers

density = [2400, 2460, 2800]

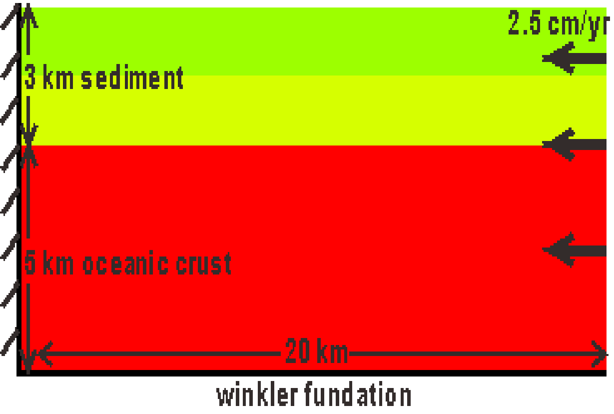

density = [2400, 2460]

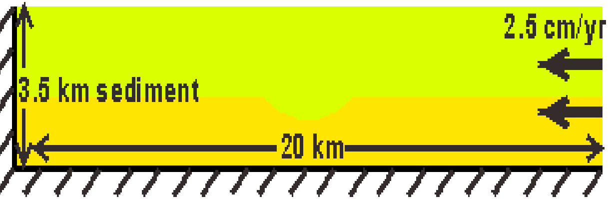

Light material

density = [2400, 1800, 2460, 2800]

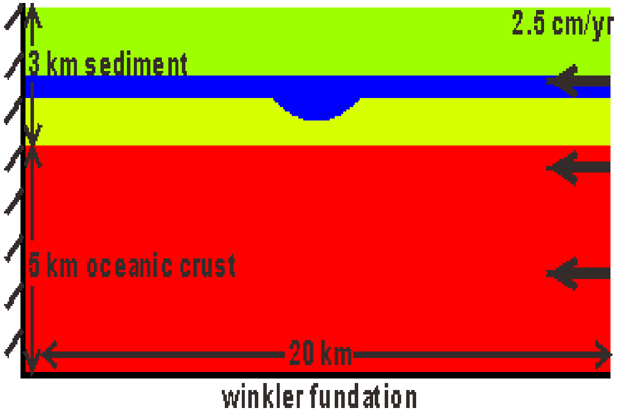

density = [2400, 1800, 2460]

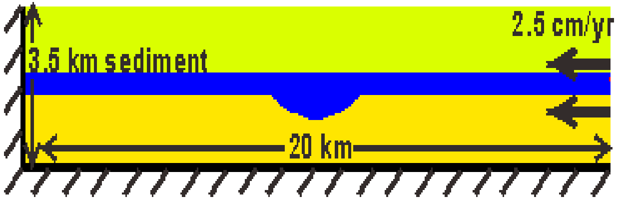

Dense material

density = [2400, 2500, 2460, 2800]

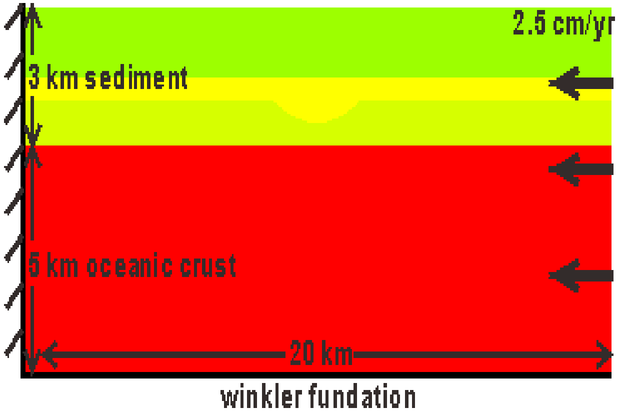

density = [2400, 2500, 2460]

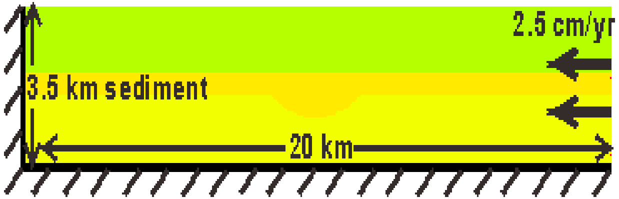

Two layers	Light material	Dense material

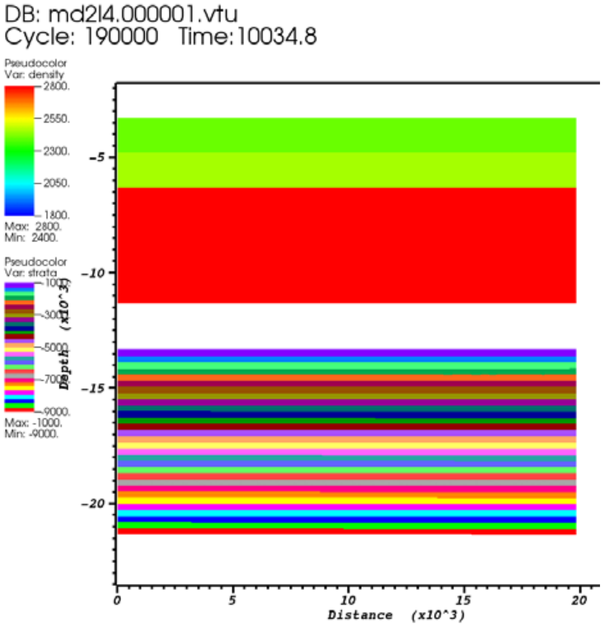

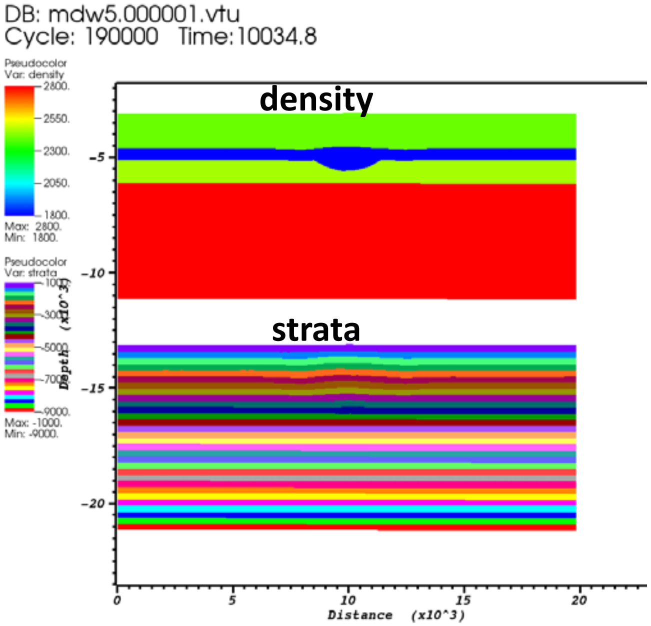

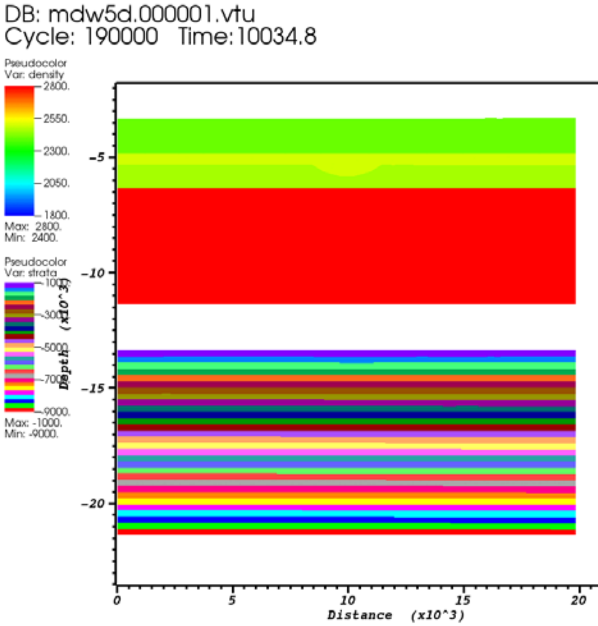

Fault and fold	Mud diapir and fault	Fault and fold

Two layers

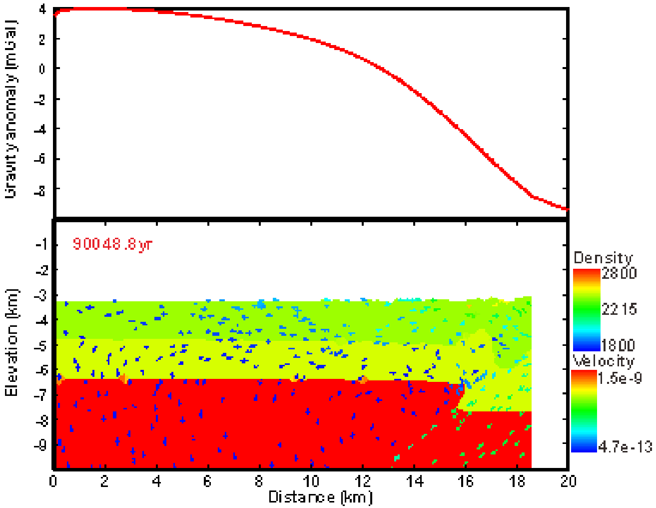

Light material

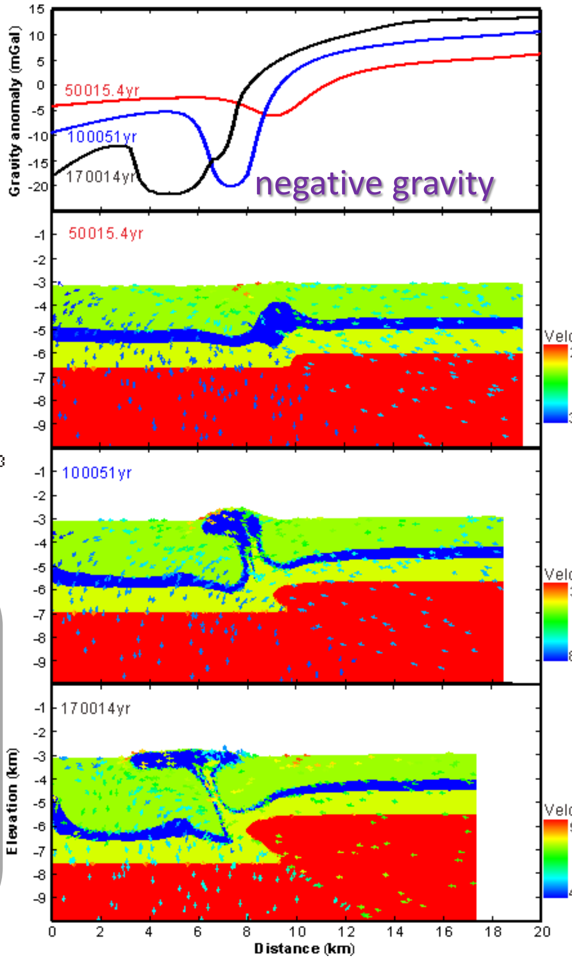

Dense material

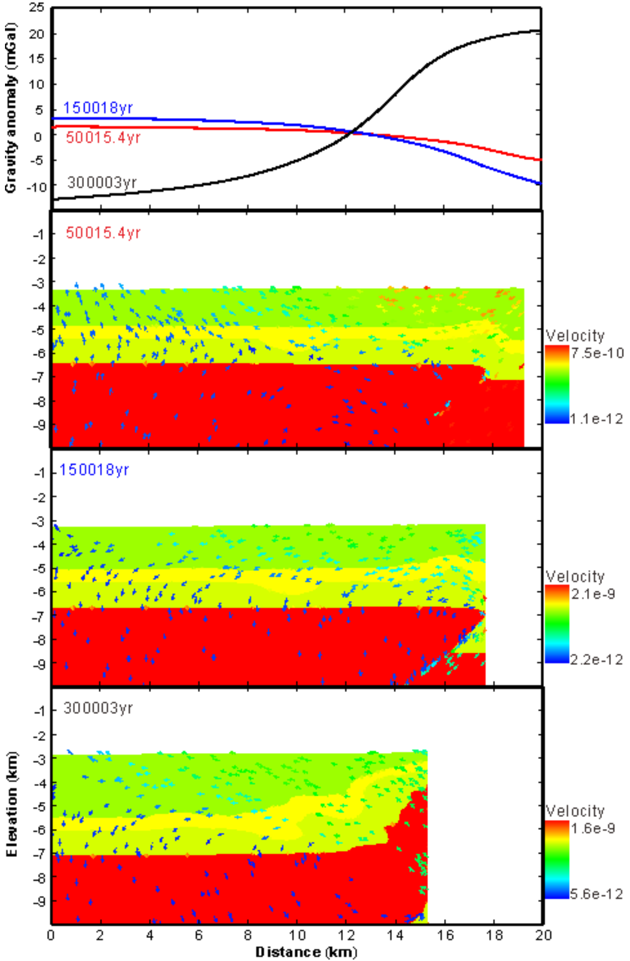

Gravity anomaly (Lowrie, 2007)

$$\Delta g_z = \sum_{c=1}^{n} \frac{2 G d_c V_c z}{x^2 + z^2}$$

G the universal gravitational constant

d_c density

V_c volume per unit length

n the number of cells

Two layers

Fold

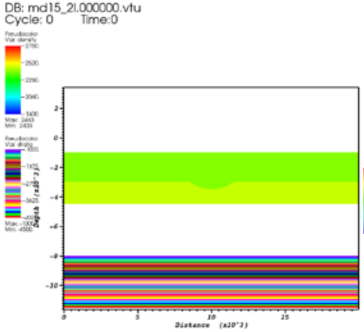

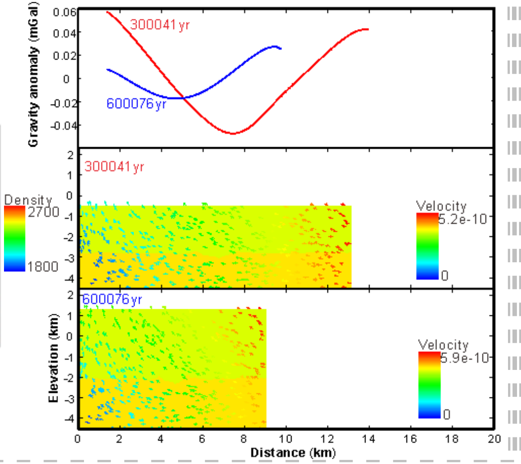

Light material

Mud diapir

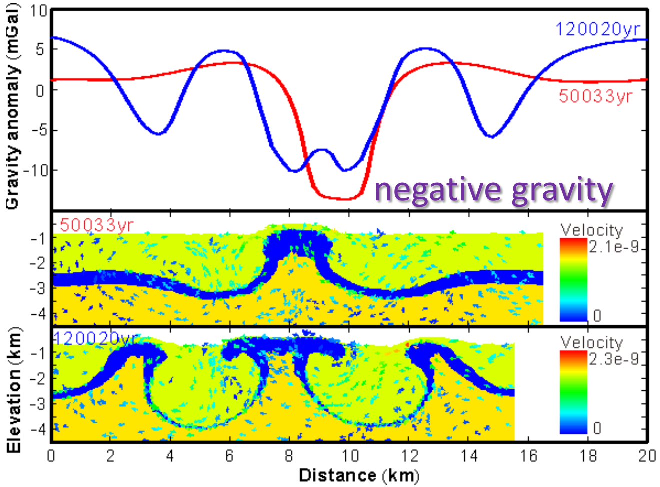

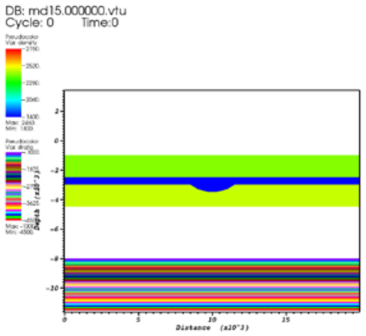

Dense material

Fold

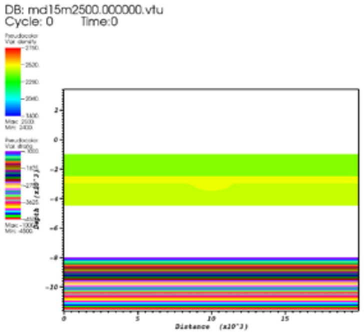

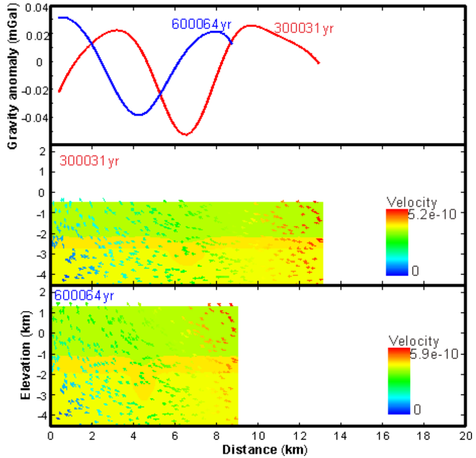

Mud diapir

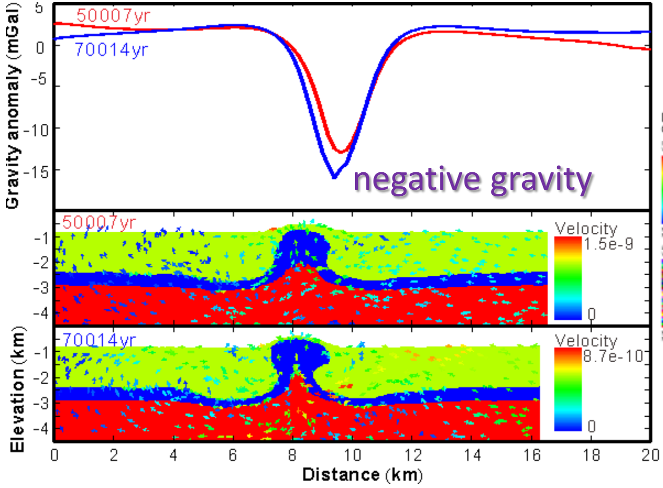

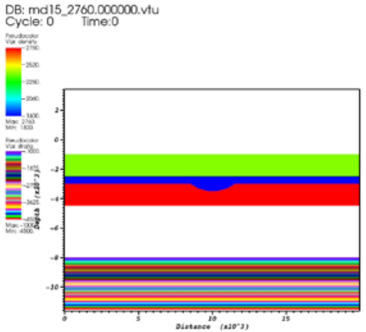

How light can develop a mud diapir?

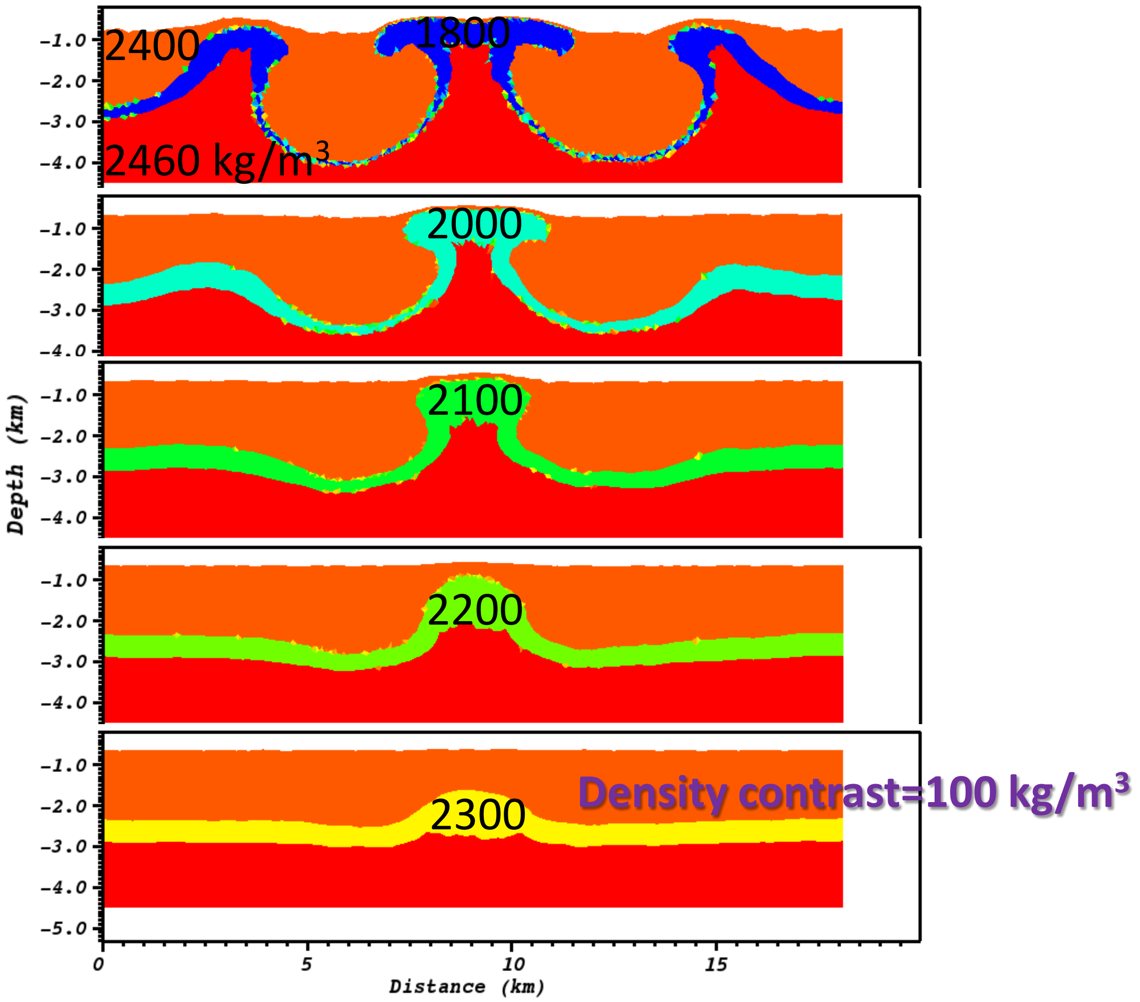

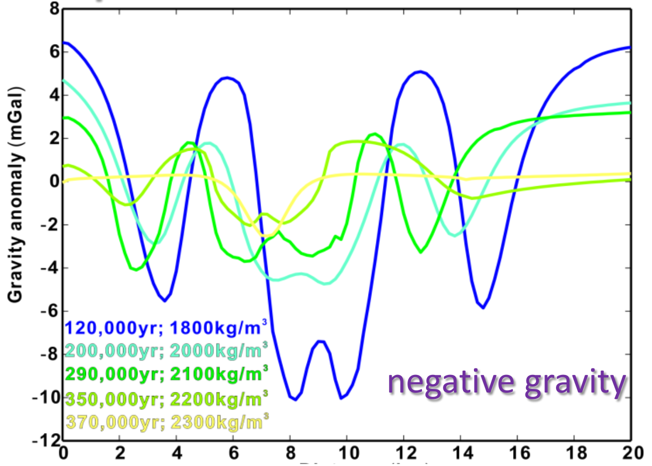

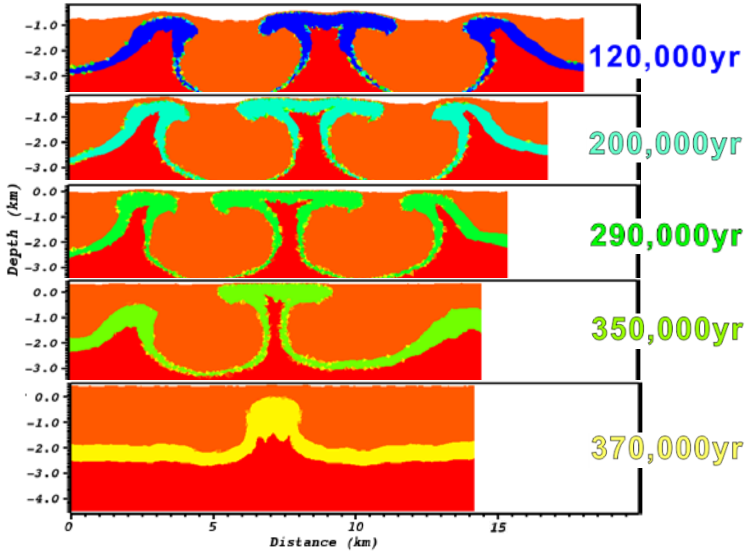

Is positive gravity from tectonic structure?

Changing bottom material with more viscous one.
Varying density of middle materials.

To increase density of bottom material -> more positive ?

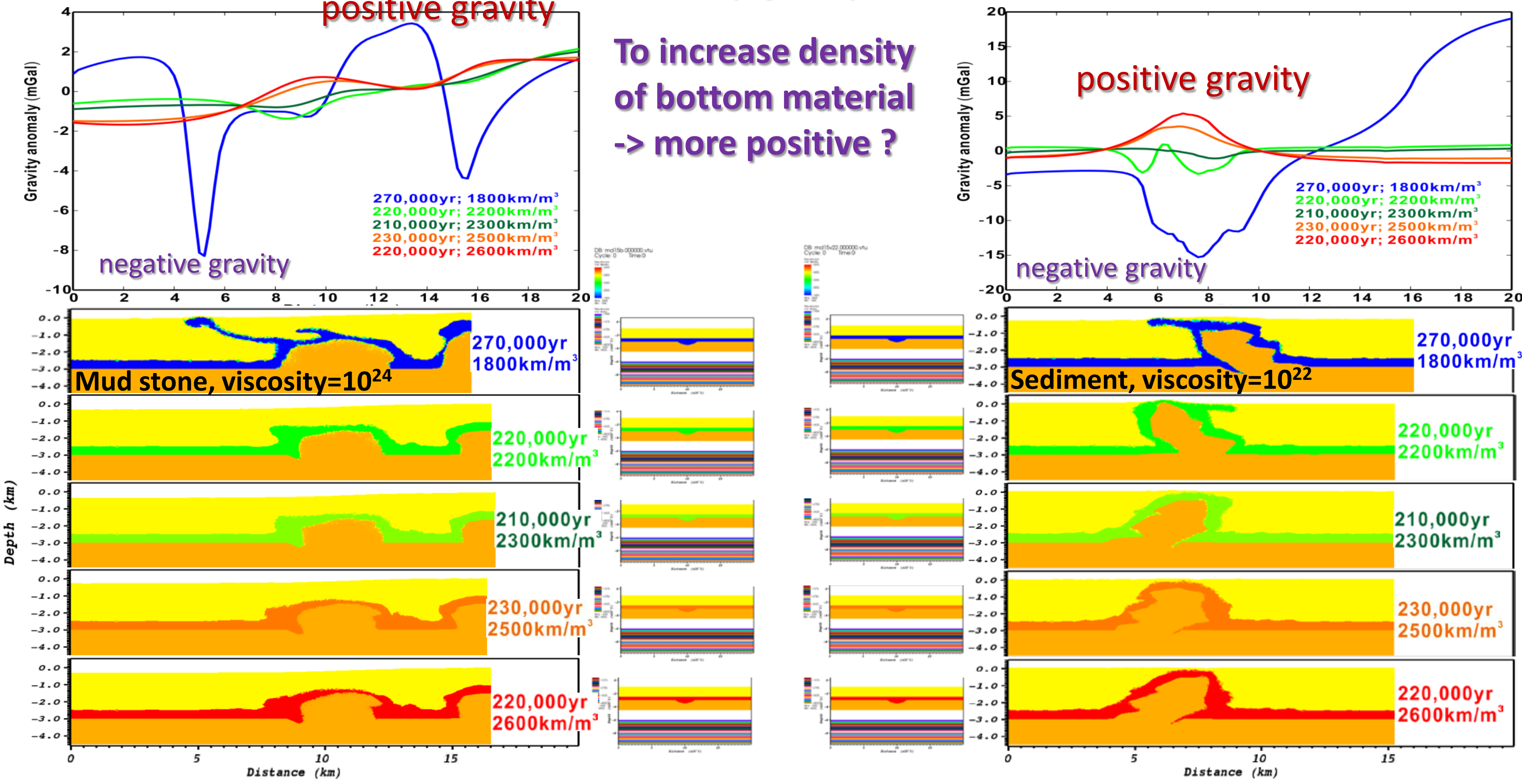

Dehydration from light material

Setting of dehydration:
Water content of light materials decrease from 0.54 to 0,
while density increase from 1800 to 2700 kg/m3.

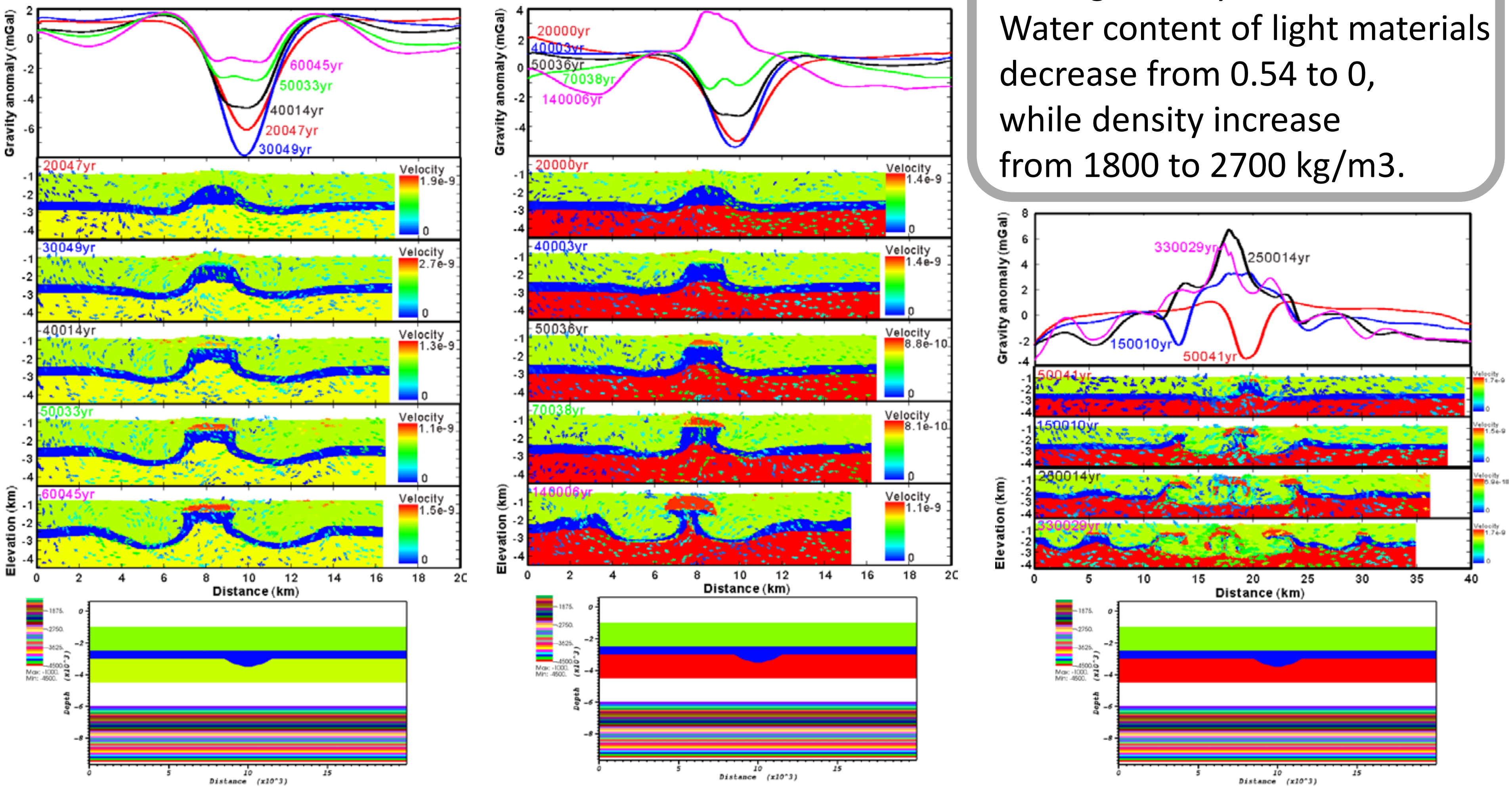

Does geometry matter?

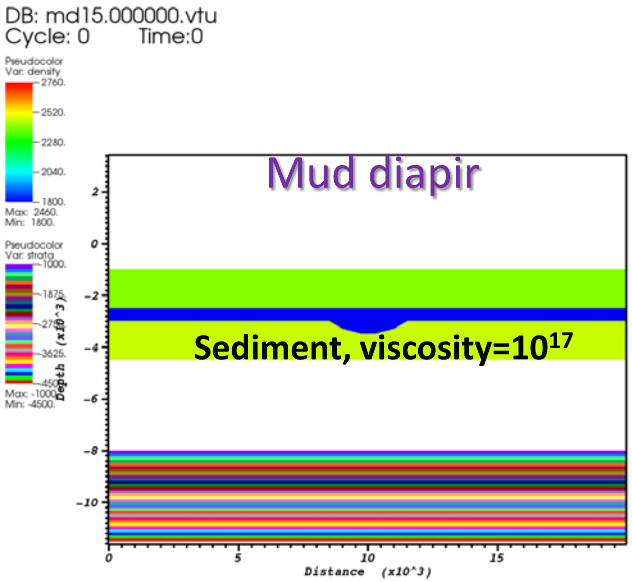

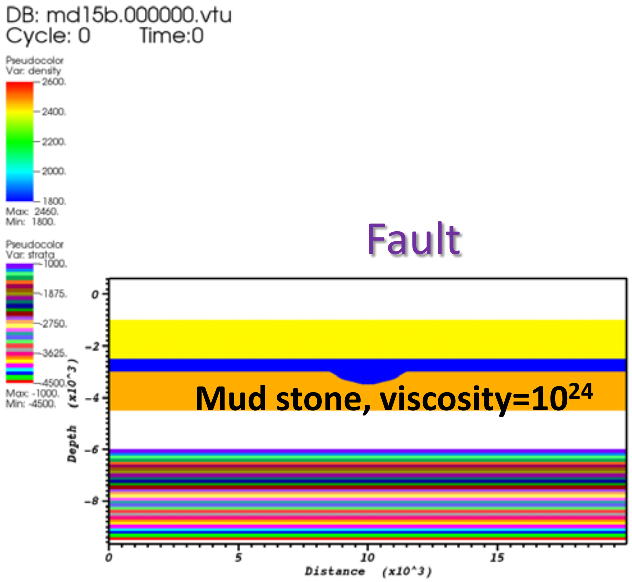

Mud diapir *take longer time*

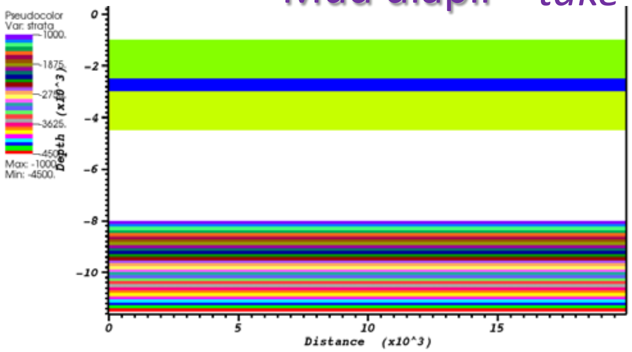

No conjugate fault Thrust

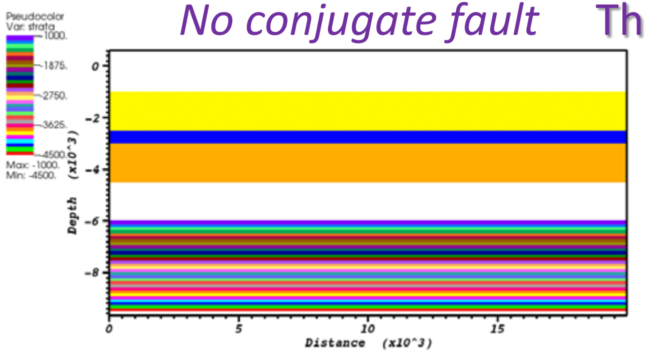

Models vs. Seismic profiles

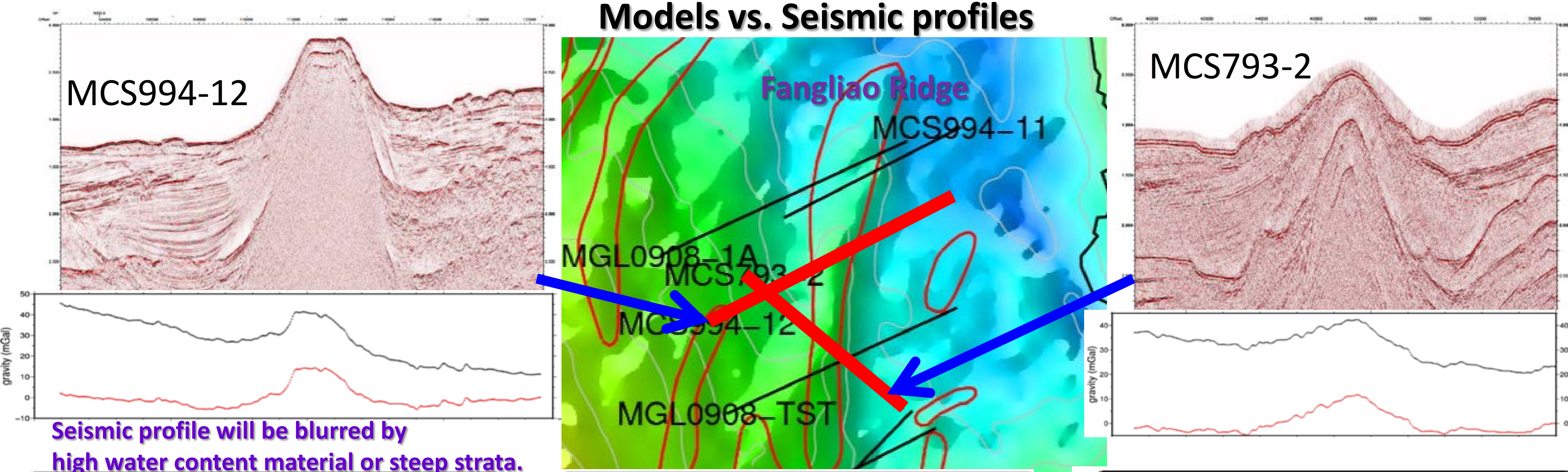

Seismic profile will be blurred by
high water content material or steep strata.

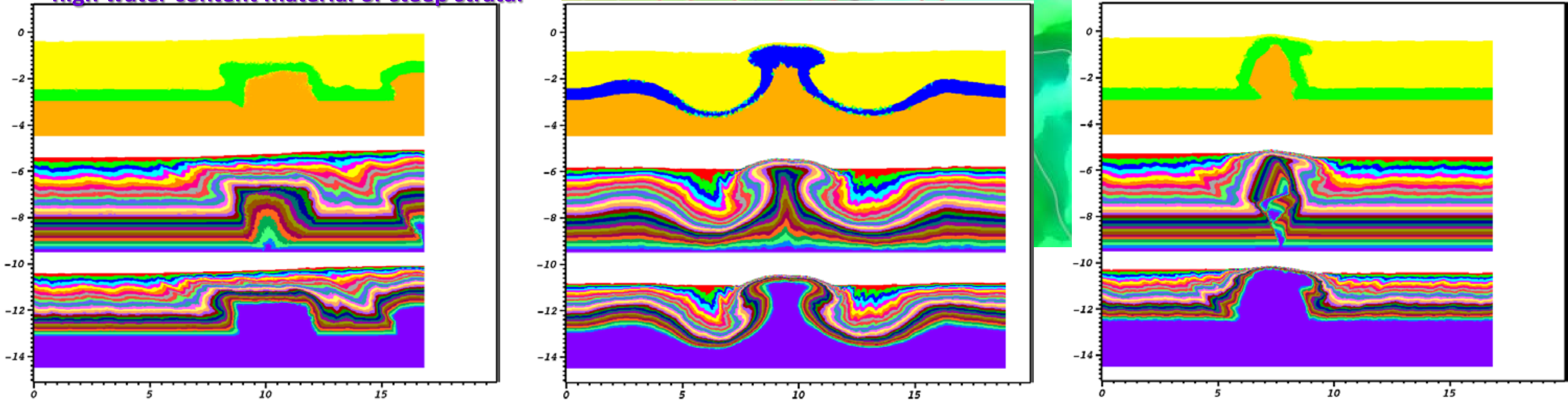

Verifying consequent gravity with the numerical modelling

- The light materials, e.g. fluid, gas, etc, can form **diapir-wise structure** penetrating srata, however which will always generate a negative gravity anomaly
- The **dense** buried materials cannot be injected into upper layers, while their folding or faulting can move parts of them to shallow levels → may have **positive** gravity anomaly
- **Dehydrated** dense **diapir-wise** materials can balance with upwelling diapirs but sink eventually → **positive** gravity anomaly

→ A clue to study the physical properties of the underlying strata, density, compaction, shear/bulk modului etc.

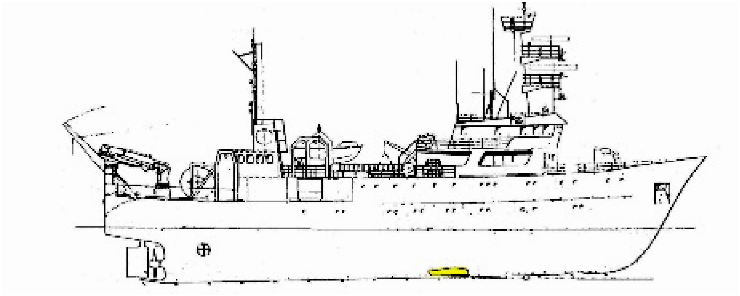

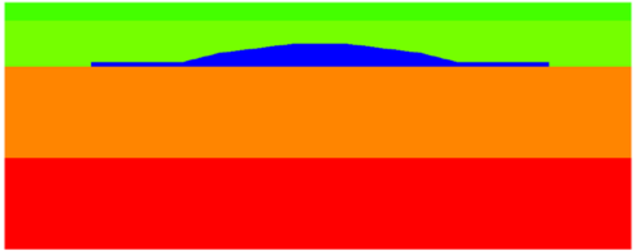

THANK YOU!

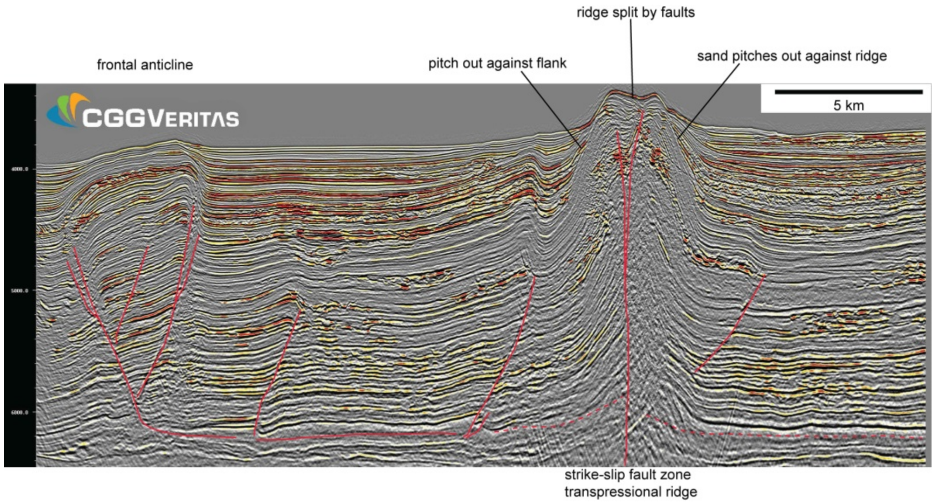
frontal anticline
pitch out against flank
ridge split by faults
sand pitches out against ridge
CGGVERITAS
5 km
strike-slip fault zone
transpressional ridge

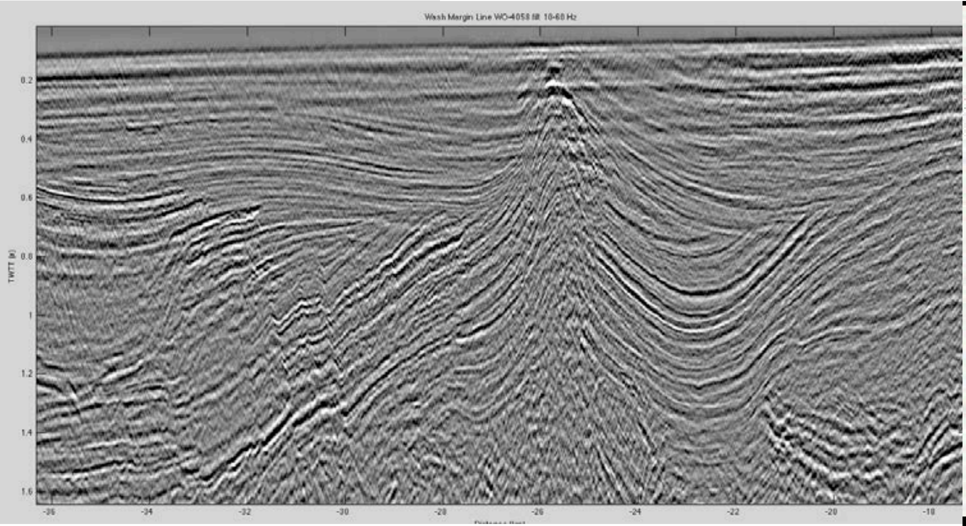
Wash Margin Line WO-4058 filt 10-60 Hz

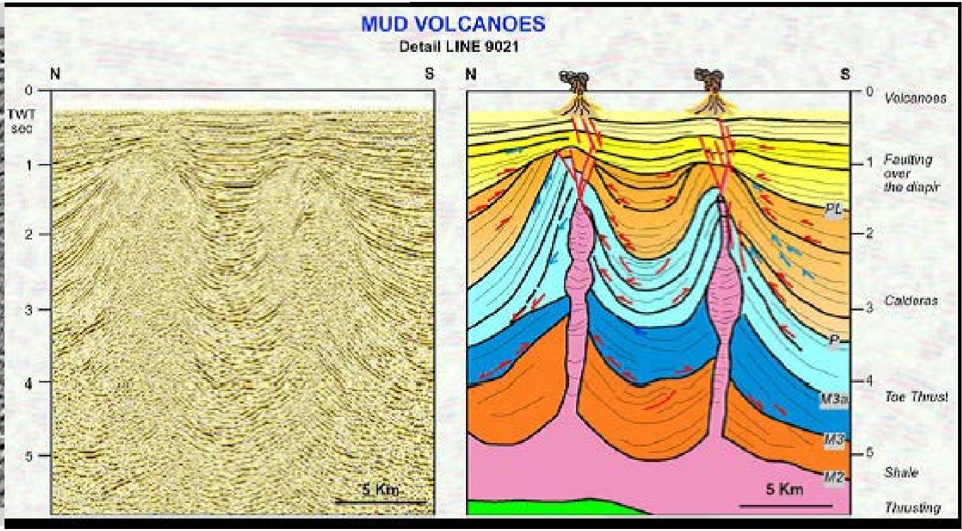
MUD VOLCANOES
Detail LINE 9021
N
S
TWT
sec
0
1
2
3
4
5
5 Km
N
S
Volcanoes
Faulting
over
the diapir
PL
Calderas
P
M3a
Toe Thrust
M3
M2
Shale
Thrusting
5 Km